Kakehashi, A. Wanibuchi, H.	carcinogens: Evidence from mechanism-based carcinogenicity studies.	Assessment		1	
Tago, Y., Wei, M., Ishii, N., Kakehashi, A. Wanibuchi, H.	Evaluation of the subchronic toxicity of dietary administered *Equisetum arvense* in F344 rats.	J Toxicol. Pathol.	23	245-251	2010
Wei, M, Wanibuchi H, Nakae D, Tsuda H, Takahashi H, Hirose M, Totsuka M, Tatematsu M, Fukushima S.	Low-dose carcinogenicity of 2-amino-3-methylimidazo[4,5-*f*]quinoline in rats: Evidence for the existence of no-effect levels and a mechanism involving p21Cip/WAF1.	Cancer Sci.	102	88-94	2011
Kakehashi, A., Ishii, N., Shibata, T., Wei, M., Okazaki, E., Tachibana, T., Fukushima, S. Wanibuchi, H.	Mitochondrial prohibitins and septin 9 are implicated in the onset of rat hepatocarcinogenesis.	Toxicol. Sci.	119	61-72	2011
Chusiri, Y., Wongpoomchai, R., Kakehashi, A., Wei, M., Wanibuchi, H., Vinitketkumnuan, U. Fukushima, S.	Non-genotoxic mode of action and possible threshold for hepatocarcinogenicity of Kojic acid in F344 rats.	Food Chem Toxicol	49	471-476	2011
Hoshi, H., Sawada, T., Uchida, M., Saito, H., Iijima, H., Toda-Agetsuma, M., Wada, T., Yamazoe, S., Tanaka, H., Kimura, K., Kakehashi, A., Wei, M., Hirakawa, K. Wanibuchi, H.	Tumor-associated MUC5AC stimulates in vivo tumorigenicity of human pancreatic cancer.	International journal of oncology	38	619-627	2011
Ishii, N., Wei, M., Kakehashi, A., Doi, K., Yamano, S., Inaba, M. Wanibuchi, H.	Enhanced urinary bladder, liver and colon carcinogenesis in Zucker diabetic fatty rats in a mulri-organ carcinogenesis: Evidence for mechanisms involving activation of PI3K signaling and impairment of p53 on urinary bladder carcinogenesis.	J Toxicol Pathol.	24	1-12	2011
Shimizu, M., Sakai, H., Shirakami, Y., Iwasa, J., Yasuda, Y., Kubota, M., Takai, K., Tsurumi, H., Tanaka, T., Moriwaki, H.	Acyclic retinoid inhibits diethylnitrosamine-induced liver tumorigenesis in obese and diabetic C57BLKS/J- +Lepr^{db}/+Lepr^{db} mice.	Cancer Prev Res	4	128-36	2011

Iwasa, J., Shimizu, M., Shiraki, M., Shirakami, Y., Sakai, H., Terakura, Y., Takai, K., Tsurumi, H., Tanaka, T., Moriwaki, H.	Dietary supplementation with branched-chain amino acids suppresses diethylnitrosamine-induced liver tumorigenesis in obese and diabetic C57BL/KsJ-*db/db* mice.	Cancer Sci	101	460-467	2010
Yasuda, Y., Shimizu, M., Shirakami, Y., Sakai, H., Kubota, M., Hata, K., Hirose, Y., Tsurumi, H., Tanaka, T., Moriwaki, H.	Pitavastatin inhibits azoxymethane-induced colonic preneoplastic lesions in C57BL/KsJ-*db/db* obese mice.	Cancer Sci	101	1701-1707	2010
Imai, K., Takai, K., Nishigaki, Y., Shimizu, S., Naiki, T., Hayashi, H., Uematsu, T., Sugihara, J., Tomita, E., Shimizu, M., Nagaki, M., Moriwaki, H.	Insulin resistance raises the risk for recurrence of stage I hepatocellularcarcinoma after curative radiofrequency ablation in HCV-positive patiens: A prospective, case- series study.	Hepatol Res	40	376-382	2010
Pitchakarn, P., Ogawa, K., Suzuki, S., Takahashi, S., Asamoto, M., Chewonarin, T., Limtrakul, P., and Shirai, T.	Momordica Charantia extract suppresses rat prostate cancer progression in vitro and in vivo.	Cancer Sci	101	2234-2240	2010
Takeshita, K., Takahashi, S., Tang, M., Seeni, A., Asamoto, M., and Shirai, T.	Hypertension is positively associated with prostate cancer development in the TRAP transgenic rat model.	Pathol Int			In press
Pitchakarn, P., Suzuki, S., Ogawa, K., Pompimon, W., Takahashi, S., Asamoto, M., Limtrakul, P., and Shirai, T.	Induction of G1 arrest and apoptosis in androgen-dependent human prostate cancer by Kuguacin J, a triterpenoid from *Momordica charantia* leaf.	Cancer Lett			In press
Iwabu, M., Yamauchi, T., Okada-Iwabu, M., Sato, K., Nakagawa, T., Funata, M., Yamaguchi, M., Namiki, S., Nakayama, R., Tabata, M., Ogata, H., Kubota, N., Takamoto, I., Hayashi, Y.K.,	Adiponectin and AdipoR1 regulate PGC-1alpha and mitochondria by Ca(2+) and AMPK/SIRT1.	Nature	464	1313-1319	2010

Yamauchi, N., Waki, H., Fukayama, M., Nishino, I., Tokuyama, K., Ueki, K., Oike, Y., Ishii, S., Hirose, K., Shimizu, T., Touhara, K., Kadowaki, T.					
Kurokawa, J., Arai, S., Nakashima, K., Nagano, H., Nishijima, A., Miyata, K., Ose, R., Mori, M., Kubota, N., Kadowaki, T., Oike, Y., Koga, H., Febbraio, M., Iwanaga, T., Miyazaki, T.	Macrophage-Derived AIM Is Endocytosed into Adipocytes and Decreases Lipid Droplets via Inhibition of Fatty Acid Synthase Activity.	Cell Metab.	11	479-492	2010
Zhou, Y., Koizumi, N., Kubota, N., Asano, T., Yuhashi, K., Mochizuki, T., Kadowaki, T., Sakuma, I., Liao, H.	Fast and accurate ultrasonography for visceral fat measurement.	Med. Image Comput. Comput. Assist Interv.	13	50-58	2010
Misu, H., Takamura, T., Takayama, H., Hayashi, H., Matsuzawa-Nagata, N., Kurita, S., Ishikura, K., Ando, H., Takeshita, Y., Ota, T., Sakurai, M., Yamashita, T., Mizukoshi, E., Yamashita, T., Honda, M., Miyamoto, K., Kubota, T., Kubota, N., Kadowaki, T., Kim, H.J., Lee, I.K., Minokoshi, Y., Saito, Y., Takahashi, K., Yamada, Y., Takakura, N., Kaneko, S.	A liver-derived secretory protein, selenoprotein p, causes insulin resistance.	Cell Metab.	12	483-495	2010
Kubota, T., Kubota, N., Kumagai, H., Yamaguchi, S., Kozono, H., Takahashi, T., Inoue, M., Itoh, S., Takamoto, I., Sasako, T., Kumagai, K., Kawai, T., Hashimoto, S.,	Impaired insulin signaling in the endothelial cells reduces insulin-induced glucose uptake by the skeletal muscle.	Cell Metab.	13	294-307	2011

Kobayashi, T., Sato, M., Tokuyama, K., Nishimura, S., Tsunoda, M., Ide, T., Murakami, K., Yamazaki, T., Ezaki, O., Kawamura, K., Masuda, H., Moroi, M., Sugi, K., Oike, Y., Shimokawa, H., Yanagihara, N., Tsutsui, M., Terauchi, Y., Tobe, K., Nagai, R., Kamata, K., Inoue, K., Kodama, T., Ueki, K., Kadowaki, T.					
Kubota, T., Kubota, N., Kumagai, H., Yamaguchi, S., Kozono, H., Takahashi, T., Inoue, M., Itoh, S., Takamoto, I., Sasako, T., Kumagai, K., Kawai, T., Hashimoto, S., Kobayashi, T., Sato, M., Tokuyama, K., Nishimura, S., Tsunoda, M., Ide, T., Murakami, K., Yamazaki, T., Ezaki, O., Kawamura, K., Masuda, H., Moroi, M., Sugi, K., Oike, Y., Shimokawa, H., Yanagihara, N., Tsutsui, M., Terauchi, Y., Tobe, K., Nagai, R., Kamata, K., Inoue, K., Kodama, T., Ueki, K., Kadowaki, T.	Impaired insulin signaling in the endothelial cells reduces insulin-induced glucose uptake by the skeletal muscle.	*Cell Metab.*	13	294-307	2011

Cancer Science
The official journal of the Japanese Cancer Association

Increase of oxidant-related triglycerides and phosphatidylcholines in serum and small intestinal mucosa during development of intestinal polyp formation in Min mice

Kazutaka Ikeda,[1,2] Michihiro Mutoh,[3] Naoya Teraoka,[3] Hiroki Nakanishi,[1,2] Keiji Wakabayashi[3,4] and Ryo Taguchi[1,2,5,6]

[1]Department of Metabolome, Graduate School of Medicine, The University of Tokyo, Tokyo; [2]Core Research for Evolutional Science and Technology Program, Japan Science and Technology Agency, Saitama; [3]Cancer Prevention Basic Research Project, National Cancer Center Research Institute, Tokyo; [4]Graduate School of Food and Nutritional Sciences, University of Shizuoka, Shizuoka; [5]Department of Biomedical Sciences, College of Life and Health Sciences, Chubu University, Aichi, Japan

(Received June 23, 2010/Revised August 24, 2010/Accepted September 12, 2010/Accepted manuscript online September 21, 2010/Article first published online October 14, 2010)

Recent epidemiological studies have shown a positive association of a high-fat diet with the risk of colon cancer. Indeed, increments in the serum levels of triglycerides (TG) and cholesterols are positively related with colon carcinogenesis. We previously reported that an age-dependent hyperlipidemic state is characteristic of Min mice, an animal model for human familial adenomatous polyposis (FAP). However, qualitative and quantitative changes of lipid metabolism are poorly understood in this state. Here, we provide detailed analysis of serum lipids in Min mice using reverse-phased liquid chromatography/electrospray ionization mass spectrometry (RPLC/ESI-MS). We also demonstrate local analysis of lipid droplets in the villi of the small intestine using laser capture microdissection and a sensitive chip-based nanoESI-MS system. As a result, oxidized phosphatidylcholines (PC) such as aldehyde and carboxylic acid types were increased, even at an early stage of intestinal polyp formation in serum. In addition, hydroperoxidizable TG precursors containing linoleic acid (18:2n-6) were deposited at the tip of the villi with aging, and these hydroperoxidized TG were also increased in serum. Meanwhile, increments of the oxidizable TG precursors in serum and small intestinal mucosa were suppressed by treatment with pitavastatin, a novel third generation lipophilic statin. These results suggest that quantitative and qualitative lipid changes such as hydroperoxidizable TG precursors are important in the course of intestinal polyp formation and oxidative stress might lead to the development of intestinal polyp formation in Min mice. (*Cancer Sci* 2011; 102: 79–87)

The incidence and mortality of colon cancer, which is associated with obesity, a high-fat diet and hyperlipidemia according to several epidemiological studies, has increased in developed countries.[1–5] We previously reported an age-dependent hyperlipidemic state in *adenomatous polyposis coli* (*Apc*)-deficient Min and *Apc*^{1309} mice, animal models of familial adenomatous polyposis (FAP).[6–8] Min mice develop large numbers of intestinal polyps due to truncation mutation in both alleles of the *Apc* gene, leading to activation of Wnt signaling to promote cell growth, which is increased by consumption of a high-fat diet.[9]

Although the direct link between *Apc*-deficiency and hyperlipidemia is yet to be clarified, it is notable that serum triglyceride (TG) levels in Min mice are almost 10 times higher than those observed in wild-type littermates (C57BL/6J) at 20 weeks of age, even though both mice were fed a non-high-fat diet, AIN-76A, including corn oil (5% of total components).[6] Both groups of mice ate almost the same amount of diet, but the mean bodyweight was 16% lower in Min mice compared with that of their wild-type littermates at 20 weeks of age, which might be due to the development of intestinal polyps. Consumption of a high-fat diet is associated with hyperlipidemia and leading obesity.[10] However, Min mice featured hyperlipidemia without a high fat-diet intake or obesity. The reasons for the pathology is correlated with decreased mRNA expression levels of lipoprotein lipase (LPL), which hydrolyzes TG into free fatty acids and monoglyceride, in the liver and small intestine.[11,12] We demonstrated that induction of LPL mRNA by peroxisome proliferator-activated receptor (PPAR)-α and -γ agonists and selective LPL-inducing agent, NO-1886, which lacks potential for activating the PPAR pathways, suppressed the hyperlipidemic status, steatosis of the liver and intestinal polyp formation.[6–8] In addition, we indicated that a number of large lipid droplets were found in the surface epithelial cells of small intestinal polyps by Oil-red O staining and electron microscopy.[13] These results suggest that lipid metabolism changes might play important roles in intestinal polyp formation, but the quantitative and qualitative changes have not been well defined in the serum and small intestine.

In this study, we examined a detailed analysis of serum lipids in Min mice using electrospray ionization-mass spectrometry (ESI-MS) coupled with reverse-phased ultra-performance liquid chromatography (UPLC).[14,15] Moreover, lipid droplets in the villi of the small intestine were collected by laser microdissection (LMD) under direct microscopic visualization and analyzed using a sensitive chip-based nanoESI-MS system by neutral loss scanning of identical fatty acyl groups from individual TG molecular species and precursor ion scanning of phosphoryl choline from individual phosphatidylcholine (PC) molecular species.[16–22] The possible lipid markers for development of intestinal polyps in Min mice are discussed. Furthermore, the relationship between the markers and polyp formation in Min mice are demonstrated by administration of pitavastatin, a novel 3-hydroxy-3-methylglutaryl coenzyme-A (HMGCoA) reductase inhibitor, which possesses pleiotropic functions including anti-inflammation and anti-oxidant functions.[23–26]

Materials and Methods

Animals. Male C57BL/6-*Apc*$^{Min/+}$ mice (Min mice) were purchased from The Jackson Laboratory (Bar Harbor, ME, USA)

[6]To whom correspondence should be addressed.
E-mail: rytagu@m.u-tokyo.ac.jp

doi: 10.1111/j.1349-7006.2010.01754.x

at 6 weeks of age and genotyped as previously reported.[27] Heterozygotes of Min strain and wild-type (C57BL/6J) mice were acclimated to laboratory conditions for 1 week. Less than five mice were housed per plastic cage with sterilized softwood chips as bedding in a barrier-sustained animal room at 24°C ± 2°C and 55% humidity on a 12 h light/dark cycle.

To investigate lipid metabolism changes, male Min mice (n = 9) and wild-type mice (n = 6) at 5 weeks of age were given AIN-76A powdered basal diet (CLEA Japan, Tokyo, Japan). Min mice (n = 3) and wild-type mice (n = 2) were killed at 10, 15 and 20 weeks of age. To examine the effects of pitavastatin ([+]-monocalcium bis [3*R*,5*S*,6*E*]-7-[2-cyclopropyl-4-(4-fluorophenyl)-3-quinolyl]-3,5-dihydroxy-6-heptenoate), which was kindly provided by Kowa Pharmaceutical Co., Ltd (Aichi, Japan), male Min mice at 6 weeks of age were given pitavastatin, which was mixed well at concentrations of 40 p.p.m. for 14 weeks in AIN-76A. Min mice with pitavastatin treatment (n = 3) and with pitavastatin untreatment (n = 3) were killed at 20 weeks of age. Food and water were available *ad libitum*. The mice were observed daily for clinical signs and mortality. Bodyweights and food consumption were measured weekly. The experimental protocol was in accordance with the guidelines for Animal Experiments in the National Cancer Center and was approved by the Institutional Ethics Review Committee for Animal Experimentation.

Materials. All solvents for HPLC or MS grade were purchased from Wako Pure Chemicals (Osaka, Japan). Deionized water was obtained from a Milli-Q water system (Millipore, Milford, MA, USA).

Extraction and isolation of serum and small intestinal mucosa lipids. Total lipids from serum and small intestinal mucosa were extracted using Bligh and Dyer's method in the following procedure:[28] serum (75 μL) and small intestinal mucosa in the proximal segments (50 mg) removed by scraping were individually homogenized with 6 mL chloroform/methanol (1:2) for 10 strokes and left for 1 h at room temperature. In this process, 1 nmol of sphingomyelin (SM) (d18:1-12:0) was added as an internal standard. Each phase separation was achieved by adding 2 mL chloroform and 2 mL water. After vortexing, the mixture was centrifuged at 1000*g*. for 10 min. The bottom organic layer containing the total lipid extract was collected and dried under a gentle stream of nitrogen, and then dissolved by 200 μL chloroform-methanol (2:1) and normalized to the serum volume and intestinal mucosa weight.

Laser capture microdissection of the small intestine. The intestinal tracts of male Min mice at 10 and 20 weeks old (n = 3) were removed and separated into the small intestine. Each small intestine was divided into the proximal segment (4 cm in length), and then opened longitudinally and fixed flat between sheets of filter paper in 10% buffered formalin for further Oil-red O

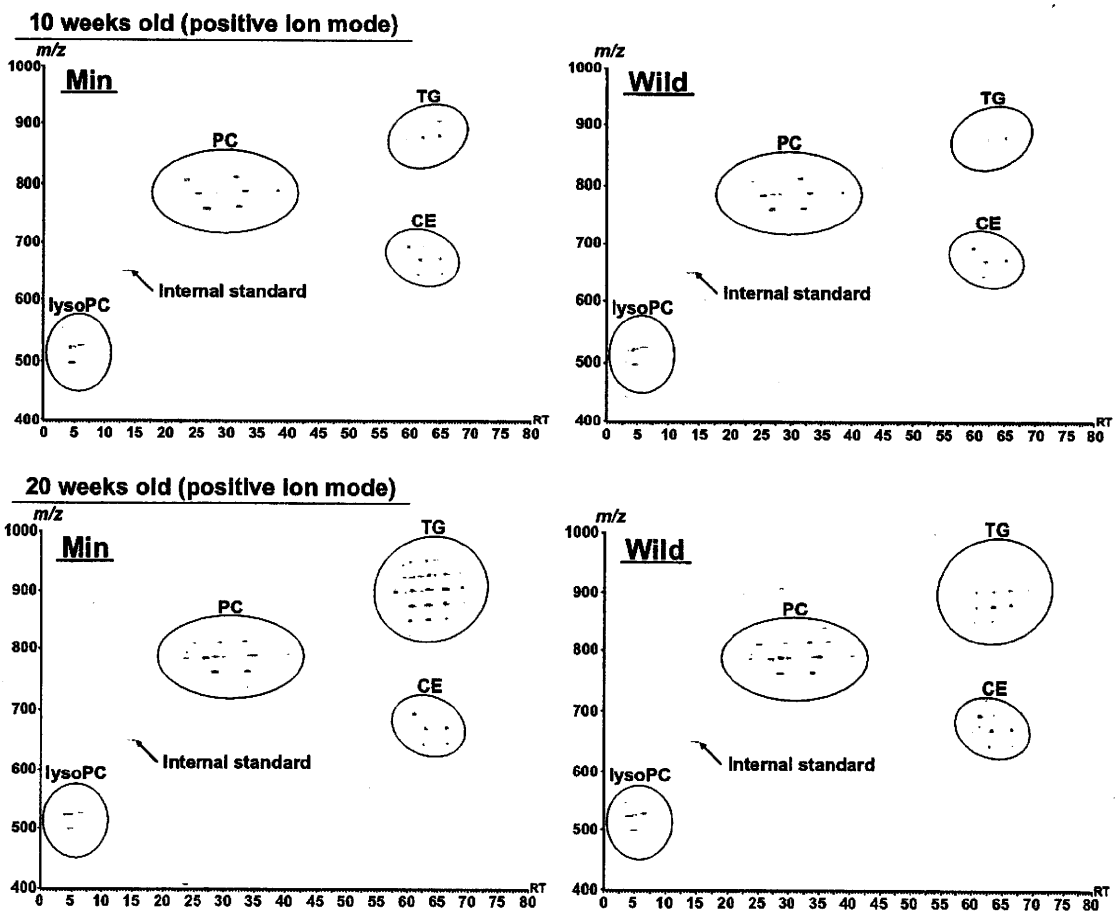

Fig. 1. 2-D profiling analysis of serum lipids from Min mice by reverse-phased liquid chromatography/electrospray ionization mass spectrometry (RPLC/ESI-MS) in positive ion mode. Each of the lipid classes was detected in the following order: lysophosphatidylcholine (lysoPC) > phosphatidylcholine (PC) > triglyceride (TG), cholesteryl ester (CE). The TG of Min mice were increased at 10 weeks of age and highly elevated at 20 weeks of age. 2-D lipid maps were constructed with X (retention time) and Y (*m/z* value) axes, and the intensity of these peaks was adjusted by color density spots.

doi: 10.1111/j.1349-7006.2010.01754.x

staining and LMD.[6] Lipid droplets of villi in the small intestine were observed using modified Oil-red O staining method for confirmation of the locus.[29] In brief, each frozen section as Swiss rolls was treated with 60% isopropanol for 1 min, and stained with Oil-red solution for 15 min at room temperature. The dye was then removed, and the section was washed with PBS and 60% isopropanol each for 2 min. For local analysis of the villi, each frozen section was mounted on DIRECTOR LMD slide (AMR Inc., Tokyo, Japan), and lipid droplets from the tip and basis of the villi were collected by Leica LMD system, LMD 6000 (Leica Microsystems, Wetzlar, Germany) with a pulsed 355-nm diode laser and individually extracted by methanol.[22] The correction intensity in each graph was calculated by the ratio of TG to the endogenous standard (16:0-18:2 PC).

Reverse-phased liquid chromatography/ESI-MS (RPLC/ESI-MS) conditions. The RPLC/ESI-MS analysis was performed using a quadrupole/time-of-flight hybrid mass spectrometer, Q-TOF micro (Waters Corporation, Milford, MA, USA) with an ACQUITY UPLC system (Waters Corporation).[14] The scan range of the instrument was set at m/z 200–1100, the scan duration of MS and MS/MS was at 0.5 s and the collision gas used for the MS/MS experiments was at 7.5×10^5 mbar (argon). The capillary voltage in positive ion mode was set at 3.5 kV, cone voltage at 30 V and collision energy of MS/MS at 30 V, whereas capillary voltage was at −2.5 kV, cone voltage at −30 V and collision energy of MS/MS at −30 V in negative ion mode.

The RPLC separation was achieved using an ACQUITY UPLC BEH C18 column (150 × 1.0 mm inner diameter [i.d.], Waters Corporation) at 45°C. Two microlitre of total lipids normalized to serum volume was individually injected. The mobile phase was acetonitrile/methanol/water : 19/19/2 (0.1% formic acid + 0.028% ammonia) (A) and isopropanol (0.1% formic acid + 0.028% ammonia) (B), and the composition was produced by mixing these solvents. The gradient consisted of holding solvent (A/B : 90/10) for 7.5 min, then linearly converting to solvent (A/B : 70/30) for 32.5 min and finally linearly converting solvent (A/B : 40/60) for 50 min. The mobile phase was pumped at a flow rate of 40–50 μL/min. The MS data processing was applied by Mass++ software (http://masspp.jp/) to detect each chromatogram peak with quantitative accuracy. The correction intensity in each graph was calculated by the ratio of TG or phosphatidylcholine (PC) to the internal standard.

Multiple reaction monitoring (MRM) conditions. The MRM analysis was performed using a quadrupole-linear ion trap hybrid mass spectrometer, 4000Q TRAP (AB SCIEX, Foster City, CA, USA) with the same ACQUITY UPLC system as previously reported.[15] Ten microlitre of total lipids normalized to serum volume was individually injected. The mobile phase was acetonitrile/methanol/water : 2/2/1 (0.1% formic acid + 0.028% ammonia) (A) and isopropanol (0.1% formic acid + 0.028% ammonia) (B), and the composition was produced by mixing these solvents. The gradient consisted of holding solvent

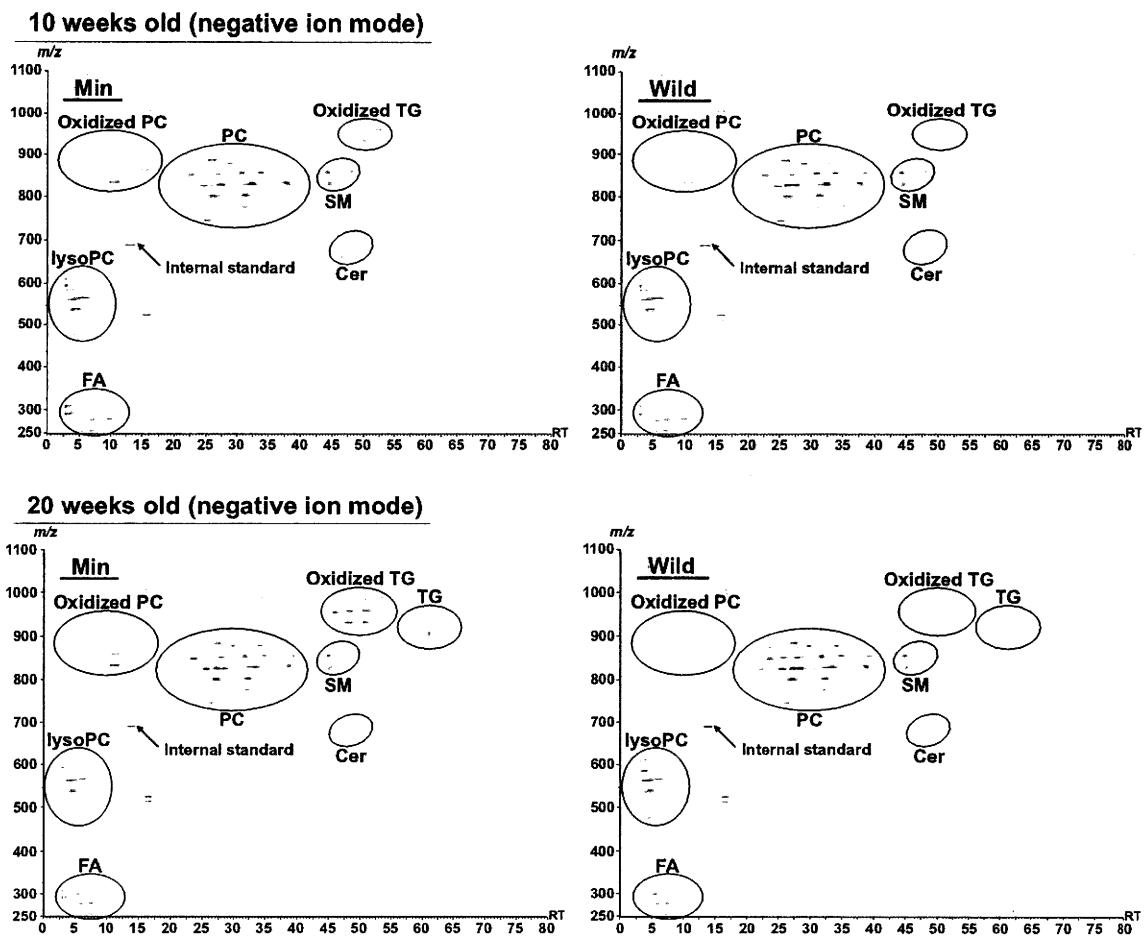

Fig. 2. 2-D profiling analysis of serum lipids from Min mice by reverse-phased liquid chromatography/electrospray ionization mass spectrometry (RPLC/ESI-MS) in negative ion mode. Each of the lipid classes was detected in the following order: oxidized phosphatidylcholine (PC), lysophosphatidylcholine (lysoPC), fatty acid (FA) > PC > sphingomyelin (SM), ceramide (Cer), oxidized triglyceride (TG) > TG. Oxidized PC and TG of Min mice were highly increased even at 10 weeks of age and highly elevated at 20 weeks of age.

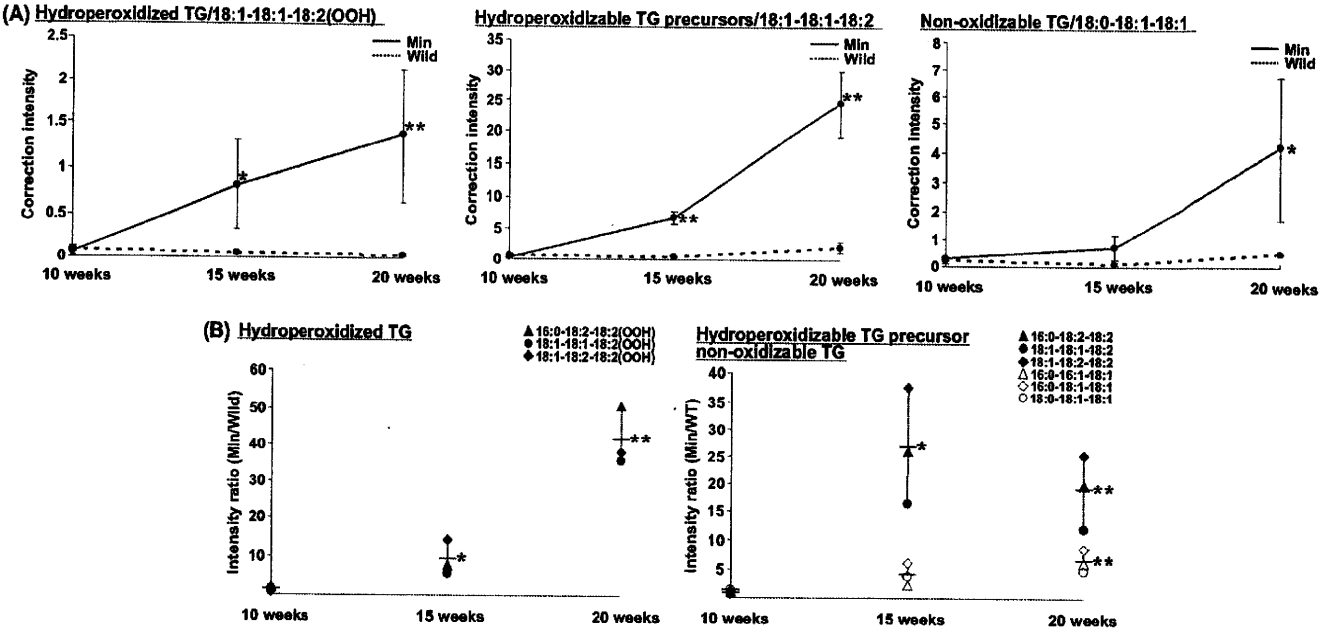

Fig. 3. Quantitative and qualitative profiles of serum triglyceride (TG) molecular species of Min mice in the course of intestinal polyp formation. (A) Compared with wild-type mice, hydroperoxidized TG and hydroperoxidizable TG precursors of Min mice were highly increased from 15 weeks of age, whereas non-oxidizable TG of Min mice were somewhat elevated at 20 weeks of age. Values are mean ± SD ($n = 3$; $^*P < 0.05$, $^{**}P < 0.01$ versus correction intensity of Min mice at 10 weeks of age). (B) Regarding ratios of Min mice to wild-type mice in serum TG molecular species, hydroperoxidized TG ratios were elevated in a time-dependent manner, and hydroperoxidized TG of Min mice at 20 weeks of age were 30–50 times larger than those of wild-type mice. Hydroperoxidizable TG precursor ratios were highly increased at 15 weeks of age and then somewhat decreased at 20 weeks of age, whereas non-oxidizable TG ratios were gradually increased in a time-dependent manner. Values are mean ± SD ($n = 3$; $^*P < 0.05$, $^{**}P < 0.01$ versus intensity ratio at 10 weeks of age) and the individual mean values of these TG are indicated by crossbars.

(A/B : 100/0) for 5 min, then linearly converting to solvent (A/B : 50/50) for 20 min and finally holding solvent (A/B : 50/50) for 34 min at a flow rate of 70 μL/min and column temperature of 30°C.

NanoESI-MS conditions. Chip-based nanoESI-MS analysis was performed using a 4000Q TRAP with chip-based ionization source, TriVersa NanoMate (Advion BioSystems, Ithaca, NY, USA). The ion spray voltage was set at 1.25 kV, gas pressure at 0.3 pound per square inch (psi) and flow rates at 200 nL/min. The scan range was set at m/z 400–1100, declustering potential at 100 V, collision energies at 50–70 V and resolutions at Q1 and Q3, "unit". The mobile phase composition was chloroform/methanol: 1/2 (0.1% ammonium formate). Total lipids were directly subjected by flow injection and selectivity analyzed by neutral loss scanning of identical fatty acyl groups from individual TG molecular species and precursor ion scanning of phosphorylcholine from individual PC molecular species.[16–21]

Statistical analysis. The student's t-test was used for statistical analysis. Values with $P < 0.05$ were considered to be statistically significant.

Results

Global analysis of serum lipids from Min mice by 2-D profiling. Intestinal polyp counts in Min mice were obviously increased with age compared with wild-type mice due to down-regulation of LPL expression. Indeed, the average number of intestinal polyps developed in Min mice was 82.4 ± 8.4 (mean ± SE). However, none of the wild-type mice developed intestinal polyps.

To further examine the effects on lipid metabolism at the molecular species level, we globally analyzed serum lipids at 10, 15 and 20 weeks of age by RPLC/ESI-MS and then created 2-D lipid maps of the individual precursor ion peaks for searching quantitative and qualitative changes. The 2-D lipid maps were constructed with X (retention time) and Y (m/z value) axes, and the intensity of these peaks was adjusted by color density spots.

As a result, TG increments in Min mice were detected on the map of positive ion mode (55–70 min) even at 10 weeks of age and were markedly found at 20 weeks of age (Fig. 1). In addition, several spots were abundantly observed on the map of negative ion mode (5–15 and 45–55 min) in Min mice compared with wild-type mice (Fig. 2). These distinctive spots were analyzed by MS/MS and respectively identified as oxidized PC and TG, which we first detected from mouse TG in white adipose tissue as previously reported.[14] At 20 weeks of age, these oxidized PC and TG were highly increased in Min mice, suggesting that enhancement of oxidative stress might be caused in the course of intestinal polyp formation.

Fig. 4. Quantitative and qualitative profiles of serum oxidized phosphatidylcholine (PC) molecular species of Min mice in the course of intestinal polyp formation. (A) Oxidized PC derived from peroxidation of polyunsaturated fatty acids (PUFA) such as linoleic acid (18:2n-6), arachidonic acid (20:4n-6) and docosahexaenoic acid (22:6n-3) at the *sn*-2 position were analyzed by multiple reaction monitoring. Aldehyde (CHO) and carboxylic acid (COOH) types of Min mice ($n = 3$) were increased even at 10 weeks of age compared with wild-type mice ($n = 2$). Values are mean ± SD. (B) In addition to these types, hydroperoxide (OOH) types of Min mice ($n = 3$) were elevated at 20 weeks compared with wild-type mice ($n = 2$). Values are mean ± SD. (C) The PC ratios of Min mice to wild-type mice were highly increased at 20 weeks of age compared with 10 weeks of age in the following order: carboxylic acid types > aldehyde types > hydroperoxide types. Individual mean values of these types are indicated by crossbars.

doi: 10.1111/j.1349-7006.2010.01754.x

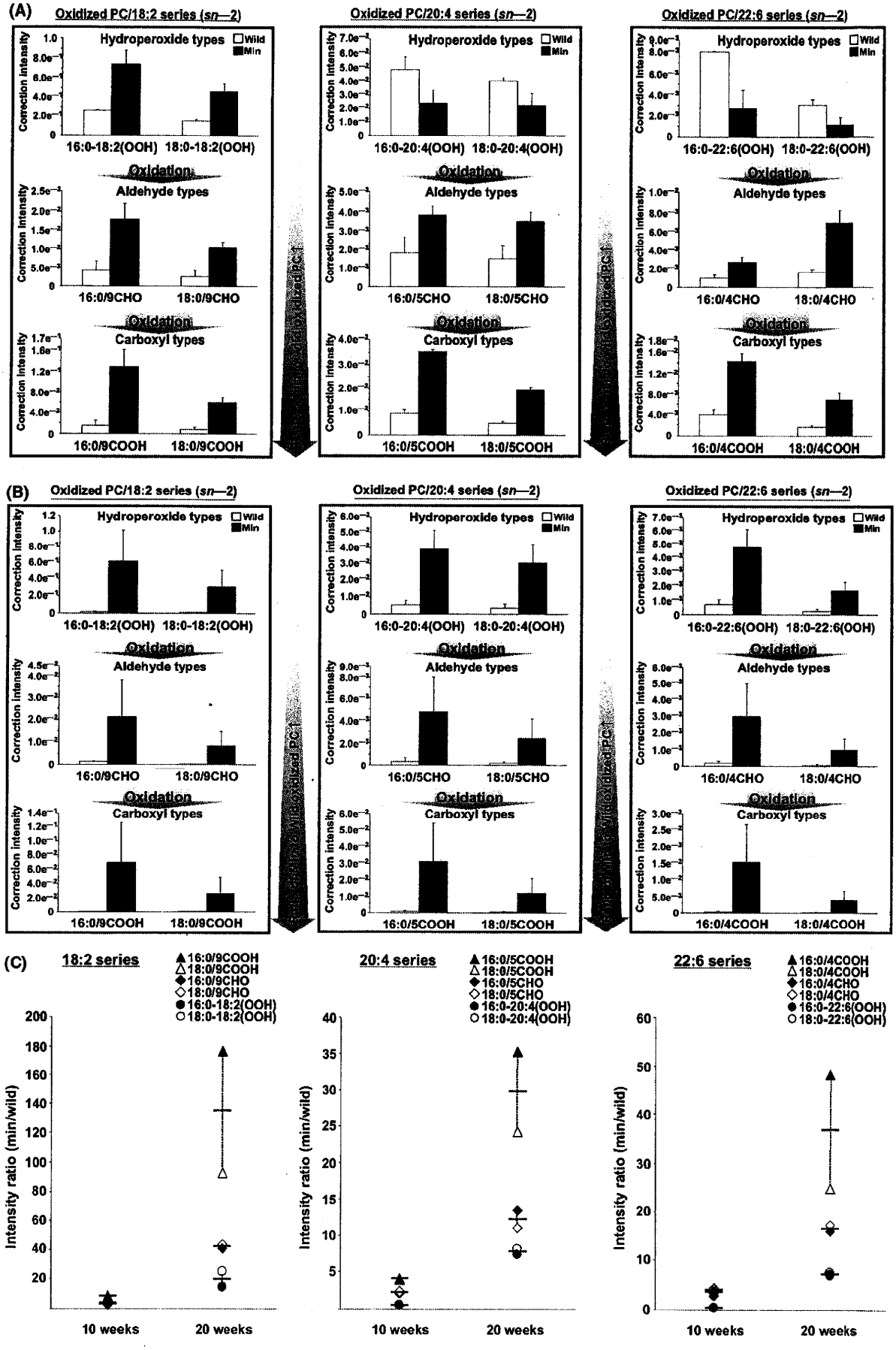

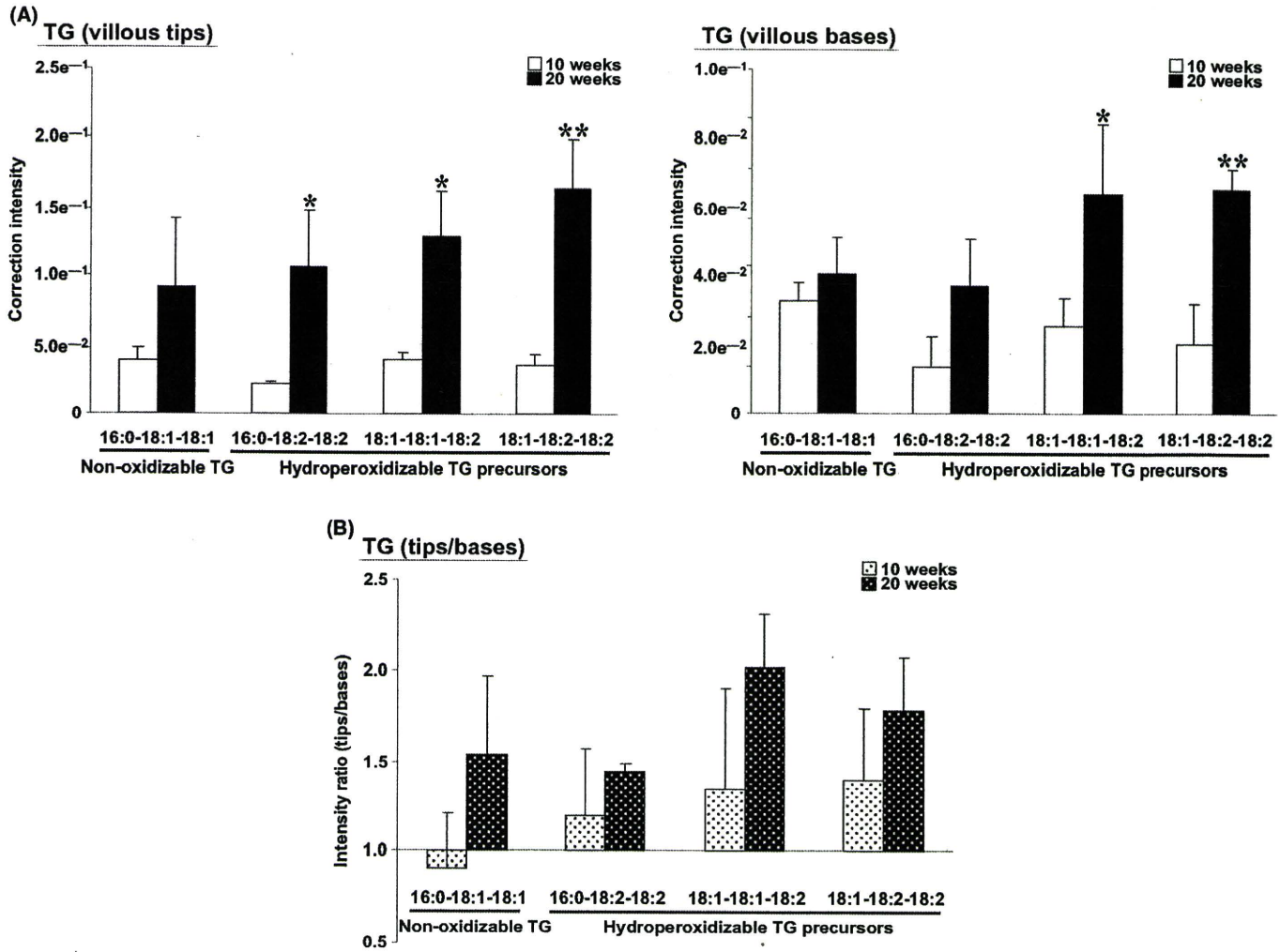

Fig. 5. Local analysis of lipid droplets in Min mice by laser microdissection and the nano-electrospray ionization-mass spectrometry (nanoESI-MS) system. (A) Hydroperoxidizable triglyceride (TG) precursors at villous tips and bases of Min mice were more increased at 20 weeks of age than 10 weeks of age. Values are mean ± SD ($n = 3$; $^*P < 0.05$, $^{**}P < 0.01$ versus correction intensity at 10 weeks of age). (B) From hydroperoxidizable TG precursor ratios of villous tips to villous bases, hydroperoxidizable TG precursors of villous tips were 1.5–2 times larger than those of villous bases at 20 weeks of age. Values are mean ± SD ($n = 3$).

Quantitative and qualitative changes of serum TG molecular species of Min mice in the course of intestinal polyp formation. These spots were more precisely quantified by Mass++, MS data processing software to detect individual chromatogram peaks with quantitative accuracy. In Min mice, serum TG molecular species such as hydroperoxidized (OOH) TG, which were derived from peroxidation of intramolecular linoleic acid (18:2n-6), and hydroperoxidizable TG precursors containing 18:2, which were oxidizable to the hydroperoxidized TG, were increased in a time-dependent manner (Fig. 3A). In particular, hydroperoxidizable TG precursors were highly elevated from 15 weeks of age. Meanwhile, non-oxidizable TG containing saturated fatty acid (SFA) and monounsaturated fatty acid (MUFA) were quantitatively unchanged until 15 weeks of age compared with wild-type mice and somewhat increased at 20 weeks of age. These results suggest that individual TG molecular species were not uniformly elevated, but oxidant-related TG were preferentially increased. As for the TG ratios of Min mice to wild-type mice, hydroperoxidized TG ratios were elevated in a time-dependent manner, and hydroperoxidized TG of Min mice at 20 weeks of age were 30–50 times larger than those of wild-type mice (Fig. 3B). Hydroperoxidizable TG precursor ratios were highly increased at 15 weeks of age and then somewhat decreased at 20 weeks of age, whereas non-oxidizable TG ratios were gradually elevated in a time-dependent manner. There were significant differences between hydroperoxidized TG ratios and non-oxidizable TG ratios at 20 weeks of age, and between hydroperoxidizable TG precursor ratios and non-oxidizable TG ratios at 15 weeks of age. It seems that these ratios might be effective indications for the pathology of intestinal polyp formation.

Quantitative and qualitative changes of serum PC molecular species of Min mice in the course of intestinal polyp formation. Regarding serum PC molecular species, hydroperoxidizable PC precursors containing 18:2 and non-oxidizable PC containing SFA were quantitatively unchanged between Min and wild-type mice at 10 and 20 weeks of age (Fig. S1). Meanwhile, oxidized PC of Min mice were abundantly observed on the 2-D map, and then a large variety of these oxidized types such as OOH, aldehydes (CHO) and carboxylic acids (COOH) were analyzed in detail by MRM with theoretically expanded data sets as previously reported.[15] These oxidized types were derived from enzymatic and non-enzymatic reactions of peroxidation of polyunsaturated fatty acids (PUFA) such as 18:2,

doi: 10.1111/j.1349-7006.2010.01754.x

arachidonic acid (20:4n-6) and docosahexaenoic acid (22:6n-3) at the *sn*-2 position and important in inflammatory biomarkers for the physiological and pathological phenomena.[30,31] Interestingly, aldehyde and carboxylic acid types derived from peroxidation of 18:2, 20:4 and 22:6 were increased even at 10 weeks of age in Min mice (Fig. 4A), indicating that oxidative stress might occur at the early stage of polyp formation. Besides these aldehyde and carboxylic acid types, hydroperoxide types were highly elevated at 20 weeks in Min mice (Fig. 4B). In addition, PC ratios of Min mice to wild-type mice in these oxidized types were increased at 20 weeks of age compared with 10 weeks of age in the following order: carboxylic acid types > aldehyde types > hydroperoxide types (Fig. 4C). These data support the ideas that Min mice at 20 weeks of age were at a high oxidative stress level and these oxidants might also be effective indications of the exacerbation stage and inflammatory state.

Local analysis of lipid droplets in the villi of Min mice. Because serum lipid contents might be affected by dietary fat absorption in the small intestine, detailed analysis of the villi were investigated at 10 and 20 weeks of age in Min mice by LMD, which permits procurement of the locus from frozen sections of Swiss-rolled middle and distal parts of the small intestines. Lipid accumulation was observed at the tip of the villi in the small intestine with Oil-red O staining and the locus was collected. These lipid mixtures were individually extracted by methanol from the collected tissues and analyzed using a chip-based nanoESI-MS system. As a result, PC molecular species were quantitatively and qualitatively unchanged at 10 and 20 weeks of age in Min mice (Fig. S2). Meanwhile, hydroperoxidizable TG precursors were more abundant at 20 weeks of age than those at 10 weeks of age in Min mice (Fig. 5A). Moreover, the TG at the tip of the villi were 1.5–2.5 times larger than those at the basis at 20 weeks of age (Fig. 5B). These results suggest that hydroperoxidizable TG precursors were comparatively deposited at the tip of the villi with age in Min mice and might be subjected to oxidative stress and inflammation in the small intestine. As discussed previously, hydroperoxidized TG and hydroperoxidizable TG precursors in the serum of Min mice were increased at 20 weeks of age, which might be caused by the increments of hydroperoxidizable TG precursors at the tip of the villi.

Suppression of hydroperoxidizable TG precursor production in the serum and small intestinal mucosa of Min mice by pitavastatin treatment. To examine the relationship between oxidative stress and polyp formation in Min mice, detailed analysis of total lipid extract from the serum and small intestinal mucosa of Min mice treated with pitavastatin at doses of 40 p.p.m. for 14 weeks were investigated by a chip-based nanoESI-MS system. Intestinal polyp formation in the pitavastatin-treated groups was significantly suppressed (the data will be presented in a separate report). The PC molecular species were quantitatively and qualitatively unchanged between the pitavastatin-treated and untreated groups (data not shown). Meanwhile, the intensity ratios of hydroperoxidizable TG precursors to non-oxidizable TG (16:0-18:1-18:1) were significantly decreased in the serum and intestinal mucosa of the pitavastatin-treated groups compared with the untreated groups (Fig. 6). These results suggest that hydroperoxidizable TG precursors are important in developing intestinal polyp formation and hydroperoxidized TG derived from the oxidizable TG precursors might induce oxidative stress and inflammation.

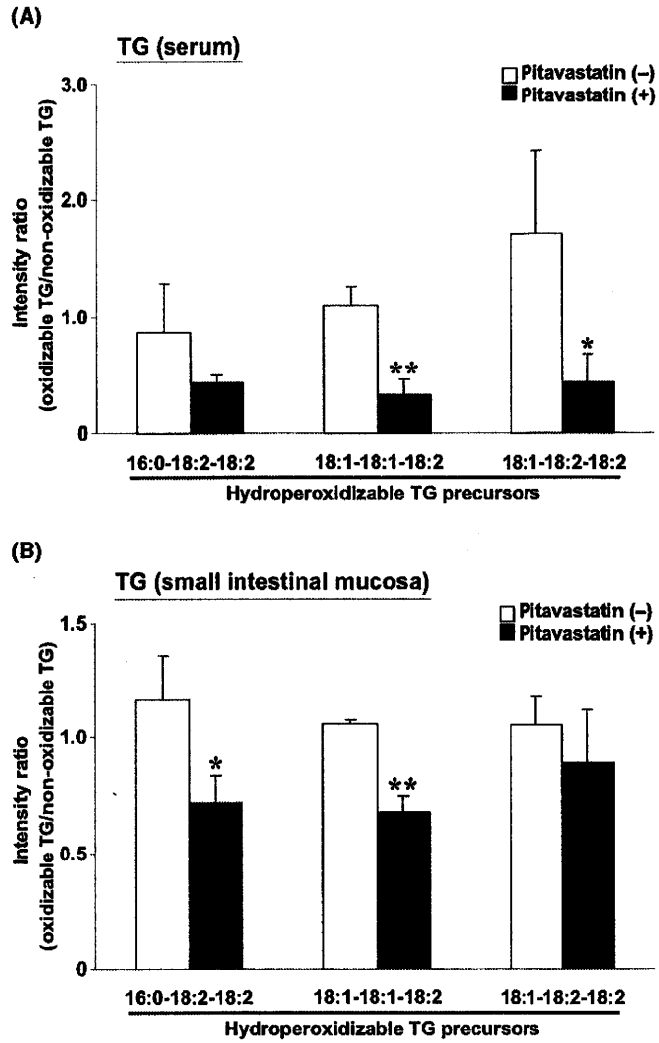

Fig. 6. Suppression of hydroperoxidizable triglyceride (TG) precursor production in serum and the small intestinal mucosa of Min mice by pitavastatin treatment. (A) Intensity ratios of hydroperoxidizable TG precursors to non-oxidizable TG (16:0-18:1-18:1) were significantly decreased in the serum of the pitavastatin-treated groups at doses of 40 p.p.m. for 14 weeks along with suppression of intestinal polyp formation compared with the untreated groups. (B) Similarly, the intensity ratios in the intestinal mucosa of the pitavastatin-treated groups were significantly reduced. Values are mean ± SD ($n = 3$; $^*P < 0.05$, $^{**}P < 0.01$ versus intensity ratios of the pitavastatin-untreated groups).

Discussion

In this study, oxidant-related TG and oxidized PC such as aldehyde and carboxylic acid types were increased even at the early stage of intestinal polyp formation in the serum of Min mice. The oxidized PC of Min mice were highly elevated even at 10 weeks of age. In particular, hydroperoxidized TG and hydroperoxidizable TG precursors were significantly increased from 15 weeks of age in a time-dependent manner. We previously reported that Min mice had higher levels of 18:2 in plasma compared with wild-type mice by gas–liquid chromatography method.[32] These results suggest that oxidant-related TG in the blood increased in the course of intestinal polyp formation, and these TG might be useful as biological markers for the formation and development of intestinal polyps.

The present study also showed that hydroperoxidizable TG precursors were comparatively deposited at the tip of villi with age in Min mice from our local analysis using LMD and sensitive chip-based nanoESI-MS system. Dietary fat mainly constituted of TG is absorbed at the tip of the villi and accumulates in the cytoplasm of intestinal epithelial cells, but not in stromal cells. The origin of the accumulated lipids seems to be derived

from the contents in the digestive tract, not from blood vessels. Therefore, our detailed analysis of the villi in Min mice is thought to be effective for directly detecting qualitative and quantitative changes. To our knowledge, local lipid analysis of the villi has not yet been reported and accumulation of hydroperoxidizable TG precursors with age was first detected in Min mice. In addition, detailed analysis of serum and the intestinal mucosa in Min mice treated with pitavastatin revealed that hydroperoxidizable TG precursors were significantly decreased along with suppression of intestinal polyp formation. It is speculated that accumulation of hydroperoxidizable TG precursors in the small intestine mucosa leads to an increased serum level of hydroperoxidized TG, and oxidative stress and inflammation might be systemically induced by these oxidized TG. For one reason, the fact that malabsorption of the hydroperoxidizable TG precursors occurs at the tip of the villi, which might evoke a source for increments of hydroperoxidized TG in serum. For another reason, hydroperoxidizable TG precursor increments at the tip of the villi lead to an elevated influx into the general circulation, and hydroperoxidized TG might be abundantly generated by peroxidation of these precursors. Moreover, hydroperoxidized TG derived from these precursors could induce DNA damage, which might link to truncation mutation in both alleles of the *Apc* gene. However, further experiments are needed to sensitively detect oxidized PC and TG from the small regions of the villi by our local analysis, and to clarify the role of hydroperoxidized TG in intestinal polyp formation.

In conclusion, hydroperoxidizable TG precursors of Min mice in serum and the small intestine mucosa were increased in the course of intestinal polyp formation, and increase of these oxidizable TG precursors was suppressed by pitavastatin. These oxidant-related lipids might be useful as biological indications for the formation and development of intestinal polyps. Furthermore, hydroperoxidized TG, hydroperoxidizable TG precursors and oxidized PC such as aldehyde and carboxylic acid types were highly increased even at 10 weeks of age, and these lipids might be possible markers for early intestinal polyp formation. These results also suggest that qualitative changes of TG and PC are important in the course of intestinal polyp formation and might lead to their development in Min mice.

Acknowledgments

The authors thank Reiko Yajima for technical assistance. This study was performed with the help of Core Research for Evolutional Science and Technology (CREST), Japan Science and Technology Agency (JST).

Disclosure Statement

The authors have no conflict of interest.

References

1 Le Marchan L, Wilkens LR, Kolonel LN, Hankin JH, Lyu LC. Associations of sedentary lifestyle, obesity, smoking, alcohol use, and diabetes with the risk of colorectal cancer. *Cancer Res* 1997; **57**: 4787–94.
2 Abu-Abid S, Szold A, Klausner J. Obesity and cancer. *J Med* 2002; **33**: 73–86.
3 Yamada K, Araki S, Tamura M *et al.* Relation of serum total cholesterol, serum triglycerides and fasting plasma glucose to colorectal carcinoma *in situ*. *Int J Epidemiol* 1998; **27**: 794–8.
4 Kaye JA, Meier CR, Walker AM, Jick H. Statin use, hyperlipidaemia, and the risk of breast cancer. *Br J Cancer* 2002; **86**: 1436–9.
5 Otani T, Iwasaki M, Ikeda S *et al.* Serum triglycerides and colorectal adenoma in a case–control study among cancer screening examinees (Japan). *Cancer Causes Control* 2006; **17**: 1245–52.
6 Niho N, Takahashi M, Kitamura T *et al.* Concomitant suppression of hyperlipidemia and intestinal polyp formation in *Apc*-deficient mice by peroxisome proliferator-activated receptor ligands. *Cancer Res* 2003; **63**: 6090–5.
7 Niho N, Takahashi M, Shoji Y *et al.* Dose-dependent suppression of hyperlipidemia and intestinal polyp formation in Min mice by pioglitazone, a PPAR gamma ligand. *Cancer Sci* 2003; **94**: 960–4.
8 Niho N, Mutoh M, Takahashi M, Tsutsumi K, Sugimura T, Wakabayashi K. Concurrent suppression of hyperlipidemia and intestinal polyp formation by NO-1886, increasing lipoprotein lipase activity in Min mice. *Proc Natl Acad Sci USA* 2005; **102**: 2970–4.
9 Mutanen M, Pajari AM, Oikarinen SI. Beef induces and rye bran prevents the formation of intestinal polyps in Apc(Min) mice: relation to beta-catenin and PKC isozymes. *Carcinogenesis* 2000; **21**: 1167–73.
10 Keys A, Menotti A, Karvonen MJ *et al.* The diet and 15-year death rate in the seven countries study. *Am J Epidemiol* 1986; **124**: 903–15.
11 Gehrisch S. Common mutations of the lipoprotein lipase gene and their clinical significance. *Curr Atheroscler Rep* 1999; **1**: 70–8.
12 Mead JR, Irvine SA, Ramji DP. Lipoprotein lipase: structure, function, regulation, and role in disease. *J Mol Med* 2002; **80**: 753–69.
13 Mutoh M, Komiya M, Teraoka N *et al.* Overexpression of low-density lipoprotein receptor and lipid accumulation in intestinal polyps in Min mice. *Int J Cancer* 2009; **125**: 2505–10.
14 Ikeda K, Oike Y, Shimizu T, Taguchi R. Global analysis of triacylglycerols including oxidized molecular species by reverse-phase high resolution LC/ESI-QTOF MS/MS. *J Chromatogr B Analyt Technol Biomed Life Sci* 2009; **877**: 2639–47.
15 Nakanishi H, Iida Y, Shimizu T, Taguchi R. Analysis of oxidized phosphatidylcholines as markers for oxidative stress, using multiple reaction monitoring with theoretically expanded data sets with reversed-phase liquid chromatography/tandem mass spectrometry. *J Chromatogr B Analyt Technol Biomed Life Sci* 2009; **877**: 1366–74.
16 Houjou T, Yamatani K, Nakanishi H, Imagawa M, Shimizu T, Taguchi R. Rapid and selective identification of molecular species in phosphatidylcholine and sphingomyelin by conditional neutral loss scanning and MS3. *Rapid Commun Mass Spectrom* 2004; **18**: 3123–30.
17 Houjou T, Yamatani K, Imagawa M, Shimizu T, Taguchi R. A shotgun tandem mass spectrometric analysis of phospholipids with normal-phase and/or reverse-phase liquid chromatography/electrospray ionization mass spectrometry. *Rapid Commun Mass Spectrom* 2005; **19**: 654–66.
18 Taguchi R, Nishijima M, Shimizu T. Basic analytical systems for lipidomics by mass spectrometry in Japan. *Methods Enzymol* 2007; **432**: 185–211.
19 Han X, Gross RW. Global analyses of cellular lipidomes directly from crude extracts of biological samples by ESI mass spectrometry: a bridge to lipidomics. *J Lipid Res* 2003; **44**: 1071–9.
20 Murphy RC, James PF, McAnoy AM, Krank J, Duchoslav E, Barkley RM. Detection of the abundance of diacylglycerol and triacylglycerol molecular species in cells using neutral loss mass spectrometry. *Anal Biochem* 2007; **366**: 59–70.
21 Ejsing CS, Sampaio JL, Surendranath V *et al.* Global analysis of the yeast lipidome by quantitative shotgun mass spectrometry. *Proc Natl Acad Sci USA* 2009; **17**: 2136–41.
22 Espina V, Wulfkuhle JD, Calvert VS *et al.* Laser-capture microdissection. *Nat Protoc* 2006; **1**: 586–603.
23 Flores NA. Pitavastatin Nissan/Kowa Yakuhin/Novartis/Sankyo. *Curr Opin Investig Drugs* 2002; **3**: 1334–41.
24 Yasui Y, Suzuki R, Miyamoto S *et al.* A lipophilic statin, pitavastatin, suppresses inflammation-associated mouse colon carcinogenesis. *Int J Cancer* 2007; **121**: 2331–9.
25 Iglesias P, Diez JJ. New drugs for the treatment of hypercholesterolaemia. *Expert Opin Investig Drugs* 2003; **12**: 1777–89.
26 Demierre MF, Higgins PDR, Gruber SB, Hawk E, Lippman SM. Statin and cancer prevention. *Nat Rev Cancer* 2005; **5**: 930–42.
27 Moser AR, Pitot HC, Dove WF. A dominant mutation that predisposes to multiple intestinal neoplasia in the mouse. *Science* 1990; **247**: 322–4.
28 Bligh EG, Dyer WJ. A rapid method of total lipid extraction and purification. *Can J Biochem Physiol* 1959; **37**: 911–7.
29 Green H, Kehinde O. An established preadipose cell line and its differentiation in culture. II. Factors affecting the adipose conversion. *Cell* 1975; **5**: 19–27.
30 Smith WL, Murphy RC. Oxidized lipids formed non-enzymatically by reactive oxygen species. *J Biol Chem* 2008; **283**: 15513–4.
31 Schneider C, Porter NA, Brash AR. Routes to 4-hydroxynonenal: fundamental issues in the mechanisms of lipid peroxidation. *J Biol Chem* 2008; **283**: 15539–43.
32 Kuriki K, Mutoh M, Tajima K, Wakabayashi K, Tatematsu M. Relationships between intestinal polyp formation and fatty acid levels in plasma, erythrocytes, and intestinal polyps in Min mice. *Cancer Sci* 2008; **99**: 2410–6.

doi: 10.1111/j.1349-7006.2010.01754.x

Supporting Information

Additional Supporting Information may be found in the online version of this article:

Fig. S1. Quantitative and qualitative profiles of serum phosphatidylcholine (PC) molecular species of Min mice in the course of intestinal polyp formation. The PC molecular species in the serum of Min mice (n = 3) were quantitatively and qualitatively similar to wild-type mice (n = 2). Values are mean ± SD. The PC containing docosahexaenoic acid (22:6n-3) was not included in the AIN-76A diet and the correction intensities were very small.

Fig. S2. Local analysis of phosphatidylcholine (PC) molecular species at the villous tips and bases of Min mice by laser microdissection and the nano-electrospray ionization-mass spectrometry (nanoESI-MS) system. The PC molecular species at the villous tips and bases of Min mice were quantitatively and qualitatively unchanged at 10 and 20 weeks of age. There was no significant difference between the villous and base values. Values are mean ± SD (n = 3). The PC containing 22:6 was not included in the AIN-76A diet and the intensities were very small.

Please note: Wiley-Blackwell are not responsible for the content or functionality of any supporting materials supplied by the authors. Any queries (other than missing material) should be directed to the corresponding author for the article.

UICC
global cancer control

IJC
International Journal of Cancer

High susceptibility to azoxymethane-induced colorectal carcinogenesis in obese KK-A^y mice

Naoya Teraoka[1], Michihiro Mutoh[1], Shinji Takasu[1], Toshiya Ueno[1], Katsuya Nakano[1], Mami Takahashi[1], Toshio Imai[2], Shuichi Masuda[3], Takashi Sugimura[1] and Keiji Wakabayashi[1,3]

[1] Cancer Prevention Basic Research Project, National Cancer Center Research Institute, Chuo-ku, Tokyo, Japan
[2] Central Animal Laboratory, National Cancer Center Research Institute, Chuo-ku, Tokyo, Japan
[3] Graduate School of Food and Nutritional Sciences, University of Shizuoka, Suruga-ku, Shizuoka, Japan

Obesity is associated with colon carcinogenesis. However, not much information is available regarding the mechanisms of obesity-associated colorectal cancer, and there are only few useful animal models for investigating the underlying mechanism between obesity and colorectal cancer. KK-A^y mice exhibit severe obesity. Amount of visceral fat assessed by micro-computed tomography was almost 15 times higher than that of same aged C57BL/6J mice. Treatment with azoxymethane (AOM; 200 μg/mouse injected once a week for 3 times) resulted in markedly increased colon aberrant crypt foci (ACF) development (≈70 ACF/mouse) in KK-A^y mice compared with lean C57BL/6J mice (≈9 ACF/mouse). Moreover, administration of AOM at a dose of 200 μg/mouse once a week for 6 times developed colorectal adenocarcinomas within only 7 weeks after the last AOM injection. The incidence of adenocarcinoma was 88% in KK-A^y mice and was markedly higher than the 4% observed in C57BL/6J mice. The number of tumors/mouse was 7.80 in KK-A^y mice and also markedly higher than the 0.12 in the C57BL/6J case. Interestingly, adenocarcinomas were observed in most of the AOM-treated KK-A^y mice along with remarkable tumor angiogenesis, and some showed submucosal invasion. These results indicate that the KK-A^y mouse, featuring intact leptin and leptin receptor Ob-Rbl, could be a useful animal model to investigate obesity-associated cancer.

Epidemiological studies have suggested that metabolic syndrome, characterized by hyperglycemia, hyperinsulinemia, hyperlipidemia and hypertension, is a risk factor for colorectal cancer.[1,2] Patients with Type 2 diabetes mellitus also have a higher risk of colon cancer.[1] In spite of a number of epidemiological studies accumulated, the mechanisms of obesity-associated colorectal cancer have not been fully understood. Moreover, there are only few useful animal models for investigating the underlying mechanism between obesity and colorectal cancer. Thus, it is very important to establish a useful animal model for this purpose.

Obesity animal models including *ob/ob* mice, *db/db* mice and Zucker rats are well established,[3–5] and it has been reported that intraperiotoneal injection of the colorectal-specific carcinogen azoxymethane (AOM) to *ob/ob* and *db/db* mice resulted in the development of around 15 colorectal aberrant crypt foci (ACF).[6] Carcinogen-induced colon carcinogenesis has also been described in Zucker rats.[7] However, these animals lack leptin or have mutation that inactivates Ob-Rbl, the long form of the leptin receptor with signaling potential.[3–5] On the other hand, short Ob-R isoforms lack major domains recruiting downstream effectors and have diminished or abolished signaling potential.[3] Evidence is accumulating that leptin can promote colorectal cancer development through activation of the NF-kappaB, Erk1/2 and PI3K/Akt pathways.[8] Therefore, it is desirable to use animals with intact leptin and leptin receptor Ob-Rbl to investigate obesity-associated colorectal cancer.

The KK-A^y mice were established by cross-mating KK mice, Type 2 diabetes model mice, with C57BL/6J-A^y mice,[9] which carry the Agouti gene (A^y), to induce severe hyperphagia, polydypsia, impaired glucose tolerance, hyperinsulinemia and hyperlipidemia[10] as compared with C57BL/6J mice, which are generally used as non-obese, non-diabetic controls.[11–13] Moreover, KK mice feature intact leptin and leptin receptor.[14]

Key words: obesity, colorectal carcinogenesis, adipocytokine
Abbreviations: ACF: aberrant crypt foci; AOM: azoxymethane; CYP2E1: cytochrome P450 2E1; GAPDH: glyceraldehyde-3-phosphate dehydrogenase; IL-6: interleukine-6; MCP-1: monocyte chemoattractant protein-1; Pai-1: plasminogen activator inhibitor-1; TNF-α: tumor necrosis factor-α; VEGF: vascular endothelial growth factor
Additional Supporting Information may be found in the online version of this article.
Grant sponsor: Grants-in-Aid for Cancer Research, Ministry of Health, Labour, and Welfare of Japan (Third-Term Comprehensive 10-Year Strategy for Cancer Control), Grants-in-Aid for Foundation for Promotion of Cancer Research
DOI: 10.1002/ijc.25711
History: Received 19 May 2010; Accepted 16 Sep 2010; Online 30 Sep 2010
Correspondence to: Michihiro Mutoh, Cancer Prevention Basic Research Project, National Cancer Center Research Institute, Chuo-ku, Tokyo, Japan, Tel.: +81-3-3542-2511, Fax: +81-3-3542-9305, E-mail: mimutoh@ncc.go.jp

In this study, we aimed to investigate the effects of the obesity on AOM-induced colorectal ACF and cancer development in KK-A^y mice. Great susceptibility to AOM-induced colorectal ACF and cancer demonstrated that the KK-A^y mouse is a good model for human metabolic syndrome. The utility of KK-A^y mice for investigation of mechanisms of how obesity enhances colorectal carcinogenesis is also discussed with reference to adipocytokine production.

Material and Methods

Animals

Female 5-week-old KK-A^y/TaJcl (KK-A^y) mice and C57BL/6J mice were purchased from CLEA Japan (Tokyo, Japan), and acclimated to laboratory conditions for 1 week. Five mice were housed per plastic cage with sterilized softwood chips as bedding in a barrier-sustained animal room at 24°C ± 2°C and 55% humidity on a 12 hr light/dark cycle and fed AIN-76A powdered basal diet (CLEA Japan). Food and water were available *ad libitum*. The animals were observed daily for clinical signs including anal bleeding and mortality. Body weights and food and water consumption were measured weekly. The experiments were performed according to the "Guidelines for Animal Experiments in the National Cancer Center" and were approved by the Institutional Ethics Review Committee for Animal Experimentation in the National Cancer Center.

AOM-induced colorectal aberrant crypt focus development

For the induction of ACF by AOM (Nard Institute, Amagasaki, Japan), 6-week-old female KK-A^y ($n = 10$) and C57BL/6J ($n = 10$) mice were given intraperitoneal injections of AOM (200 μg/mouse) once weekly for 3 weeks. Five mice each were also injected with saline as a control group. At the end of the experimental period, the colorectum was removed, opened longitudinally and fixed flat between sheets of filter paper in 10% buffered formalin for more than 24 hr. They were divided into the proximal segment, rectum (1.5 cm in length), then the proximal (middle) and distal halves of the remainder. These were stained with 0.2% methylene blue (Merck, Darmstadt, Germany) and the mucosal surface was assessed for ACF with a stereoscopic microscope, as previously reported.[15]

AOM-induced colorectal tumor development

Six-week-old female KK-A^y ($n = 25$) and C57BL/6J ($n = 25$) mice were given intraperitoneal injections of AOM (200 μg/mouse) once weekly for 6 weeks for induction of colorectal tumors. Five mice each were also injected with saline as a control group. All the mice were anesthetized with ether and sacrificed at the age of 19 weeks, because bloody stool then became frequently observed. The colorectum was opened longitudinally and colorectal tumors were noted for their location, number and size. Colorectal tumors along with nontumorous parts were fixed in 10% buffered formalin and embedded in paraffin blocks for histopathological evaluation. Diagnosis of colorectal tumors using hematoxylin and eosin (H&E) stained sections was performed according to the classification of Pozharisski.[16] The organs, including heart, kidney, liver, lung, pancreas and spleen, were also excised and were also observed macroscopically and blood samples from the abdominal aorta were collected. Abnormal findings were further histopathologically examined. Serum levels of triglyceride, total cholesterol and lipoproteins were measured as reported.[17] Blood glucose was measured using a GR-102 blood glucose monitor (Terumo, Tokyo, Japan).

Analysis of visceral adiposity

The volume and distribution of visceral fat were measured by LaTheta® X-ray computed tomography (CT; Aloka, Tokyo, Japan) from the first lumbar vertebra to the pubic bone, under inhalation anesthesia of isoflurane and were analyzed by visualization LaTheta® software as previously reported.[18]

Analysis of mRNA levels and serum adipocytokine levels

Visceral adipose tissue and colon mucosa of KK-A^y and C57BL/6J mice were rapidly deep-frozen in liquid nitrogen and stored at −80°C. Total RNA was isolated from tissue by using an RNeasy® Lipid Tissue mini kit (Qiagen, Hilden, Germany) according to the manufacture's protocol, and treated with DNase I (Invitrogen, Carlsbad, CA). One-μg RNA in a final volume of 20 μL were used for synthesis of cDNA using an Omniscript® RT Kit (Qiagen, Hilden, Germany) with an oligo (dT) primer. Real-time PCR was carried out using a DNA Engine Opticon™ 2 (MJ Japan, Tokyo, Japan) with SYBR Green Real-time PCR Master Mix (Toyobo Co., Osaka, Japan). Primers for mouse adiponectin (5′ primer- AGGATGCTACTG TTGCAAGCTCTC, 3′ primer- CAGTCAGTTGGTATCATGG TAGAG), glyceraldehyde-3-phosphate dehydrogenase (GAPDH) (5′ primer- TTGTCTCCTGCGACTTCA, 3′ primer- CACCAC CCTGTTGCTGTA), interleukine-6 (IL-6) (5′ primer- ACAAC CACGGCCTTCCCTACTT, 3′ primer- CACGATTTCCCAGA GAACATGTG), leptin (5′ primer- CCAAAACCCTCATCAA GACC, 3′ primer- GTCCAACTGTTGAAGAATGTCCC), monocyte chemoattractant protein-1 (MCP-1) (5′ primer- CCACTCACCTGCTGCTACTCAT, 3′ primer- TGGTGATC CTCTTGTAGCTCTCC), Ob-Rbl (5′ primer- CCATCTTTTA TATGATCTGCCTGAAGT, 3′ primer- TGCATTGGACAGT CTGAAAGCT), plasminogen activator inhibitor-1 (Pai-1) (5′ primer- ACAGCCTTTGTCATCTCAGCC, 3′ primer- AGGGTTGCACTAAACATGTCAG) and tumor necrosis factor-α (TNF-α) (5′ primer- TGTGCTCAGAGCTTTCAACAAC, 3′ primer- GCCCATTTGAGTCCTTGATG) were used.[19–22] To assess the specificity of each primer set, amplicons generated from the PCR reaction were analyzed for melting curves.

Serum insulin, IL-6, leptin, Pai-1, resistin and TNF-α were measured using Multiplex kits (Linco plex, St. Louis, MO).

Immunohistochemical analysis of infiltrated macrophages in visceral fat tissues

Visceral fat tissues, represented by peri-uterine and peri-ovarian white adipose tissues from KK-A^y and C57BL/6J mice were

fixed in 10% buffered formalin, embedded, and sectioned for further immunohistochemical examination with the avidin-biotin complex immunoperoxidase technique. As the first antibody, goat polyclonal anti-F4/80 antibody (R&D Systems, Minneapolis, MN) was used at 100× dilution. As the secondary antibody, biotinylated anti-goat IgG (Vector Laboratories, Burlingame, CA) was used at 200× dilution. Staining was performed using avidin-biotin reagents (Vectastain ABC reagents; Vector Laboratories, Burlingame, CA), 3,3′-diaminobenzidine and hydrogen peroxide, and the sections were counterstained with hematoxylin to facilitate orientation. Three different areas of tissue from each animal ($n = 5$) were photographed in 20× magnification, and the numbers of F4/80 positive cells were counted manually.

Analysis of crypt length and cells/crypt

The crypt length and the number of cells/crypt were evaluated on H&E stained sections from similar distal parts of nontumorous mucosa of 19 weeks KK-A^y and C57BL/6J mice with AOM treatment. Three different crypts from each animal ($n = 5$) were photographed in 40× magnification, and the crypt length were measured and the number of cells/crypt were counted.

Analysis of hepatic CYP2E1 activity

Liver microsomes were prepared from liver samples from 19-week-old KK-A^y and C57BL/6J mice with or without AOM treatment ($n = 5$ each), and cytochrome P450 2E1 (CYP2E1) activity of liver microsomes was measured using the method described by Bonnefoi *et al.*[23] with some modifications. CYP2E1 activity was expressed as the formation rate of 6-hydroxychlorzoxazone from chlorzoxazone. Mixture of 100 μg microsomes, 20 μL of 500 mM phosphate buffer (pH 7.4) and 20 μL of 500 μM chlorzoxazone solution were preincubated for 5 min at 37°C (total volume: 180 μL). Then, 20 μL of NADPH-generating system (100 mM $MgCl_2$, 10 mM NADP, 100 mM G-6-P, and 1000 U/mL G-6-PDH) were added and incubated for 5 min at 37°C. After incubation, the reaction was stopped by adding 100 μL of ice-cold acetonitrile. The concentration of formed 6-hydroxychlorzoxazone in each solution was determined with HPLC equipped with a model LC-6A pump (Shimadzu Co., Kyoto, Japan) and a model SPD-6AV UV detector (Shimadzu Co.). A UV wavelength of 295 nm was used. Each sample was chromatographed on a CAPCELL PAK C-18-UG120 (4.6 mm i.d., 150 mm in length, Shiseido Co., Tokyo, Japan). The flow rate was 1.0 mL/min. The mobile phase was a mixture of acetonitrile and 20 mM acetate buffer (pH 4.5) (30/70, v/v).

Statistical analysis

The results are expressed as mean ± standard deviation (SD) or standard error (SE) values. The significance of difference in the incidence of AOM-induced mouse tumors was analyzed using the χ^2 test and other statistical analyses were performed with Student's *t*-test. Differences were considered to be statistically significant at $p < 0.05$.

Results

Obese status observed in KK-A^y mice

The average body weights at 6 weeks of age of female KK-A^y and C57BL/6J mice were 22.9 ± 0.9 g (mean ± SD) and 17.4 ± 0.8 g, respectively, before AOM treatment. At 13 weeks of age (ACF experiment), the average body weights of KK-A^y and C57BL/6J mice with AOM treatment were 40.6 ± 2.7 g (mean ± SD) and 21.4 ± 1.5 g, and food intake were 4.0 ± 0.5 g/mouse/day and 3.0 ± 0.2 g/mouse/day, respectively. At 19 weeks of age (colorectal cancer experiment), the average body weights of KK-A^y and C57BL/6J mice with AOM treatment were 55.4 ± 4.9 g and 25.2 ± 1.5 g, and food intake were 5.2 ± 0.5 g/mouse/day and 3.6 ± 0.4 g/mouse/day, respectively. The average body weights of mice treated with AOM were slightly decreased compared with saline-treated mice. Thus, body weights of KK-A^y mice were almost twice as much as those of C57BL/6J mice. Furthermore, liver weights in KK-A^y mice were increased 1.7-fold compared to those of C57BL/6J mice.

The data of serum lipids, glucose and insulin are summarized in Supporting Information Table S1. At 13 weeks of age, the average serum levels of triglyceride, total cholesterol, free fatty acid and insulin of KK-A^y mice with AOM treatment were 484.1 ± 106.1 mg/dL (mean ± SD), 101.6 ± 12.5 mg/dL, 1796 ± 493 μEq/L and 10.1 ± 3.9 μg/mL, respectively. These levels of KK-A^y mice with AOM treatment were significantly higher ($p < 0.01$) than those of C57BL/6J mice with AOM treatment. At 19 weeks of age, the average serum levels of triglyceride, total cholesterol, free fatty acid, glucose and insulin of KK-A^y mice with AOM treatment were also significantly higher ($p < 0.01$) than those of C57BL/6J mice with AOM treatment.

As shown in Figures 1*a* and 1*b*, the subcutaneous area (indicated in yellow) and visceral area (in red) of abdominal fat in KK-A^y and C57BL/6J mice with AOM treatment could be distinguished in CT images, and subcutaneous, visceral and total amount of fat tissue were calculated individually by instrumental software. The values in all cases were significantly increased ($p < 0.01$) in KK-A^y mice compared with those of C57BL/6J mice at 13 and 19 weeks of age (Supporting Information Table S2). Notably, a marked increase was observed in the visceral fat of KK-A^y mice, such as 7.6 ± 1.1 g/mouse (at 13 weeks of age) and 11.3 ± 2.3 g/mouse (at 19 weeks of age).

Histopathological examination of visceral adipose tissue clearly showed enlargement of adipocytes (Figs. 1*c* and 1*d*), which was confirmed by quantification of the number of adipocyte nuclei observed in the field of fat tissue in KK-A^y mice (Fig. 1*e*). Immunohistochemical examination of adipose tissue with F4/80 antibody showed a 2.3-fold increase of infiltrated macrophages into the adipose tissue in KK-A^y mice compared with those of C57BL/6J mice (Fig. 1*f*). Furthermore, liver steatosis, hypertrophy of pancreatic islets and fatty infiltration in the pancreas were observed in KK-A^y mice (data not shown).

Levels of adipocytokines in serum and visceral fat tissue

Table 1 summarizes data on serum adipocytokine levels in KK-A^y and C57BL/6J mice at 13 weeks and 19 weeks. IL-6 and leptin were significantly increased ($p < 0.01$) in KK-A^y mice compared with C57BL/6J mice with AOM treatment at 13 weeks and 19 weeks. At 13 weeks, Pai-1 and resistin were significantly increased in KK-A^y mice compared with C57BL/6J mice. Meanwhile, at 19 weeks, Pai-1 and resistin had tendency to increase in KK-A^y mice compared with C57BL/6J mice. Serum TNF-α level was not significantly different between KK-A^y mice and C57BL/6J mice.

Figures 2*a* (13 weeks) and 2*c* (19 weeks) show expression levels of adipocytokines in visceral fat tissue, and MCP-1, Pai-1, TNF-α and leptin were significantly increased in KK-A^y mice at 13 weeks and 19 weeks compared with C57BL/6J mice with AOM treatment. Significant increase of IL-6 level was observed at 13 weeks, but not 19 weeks. The level of adiponectin was decreased 40% ($p < 0.05$) at 19 weeks, which was not significant at 13 weeks (Figs. 2*b* and 2*d*). Expression levels of Ob-RH in the colon of KK-A^y and C57BL/6J mice with AOM treatment at 19 weeks were measured by real-time PCR, and it was found that the levels were slightly lower in KK-A^y mice ($n = 7$) than in C57BL/6J mice ($n = 7$), but the differences were not statistically significant.

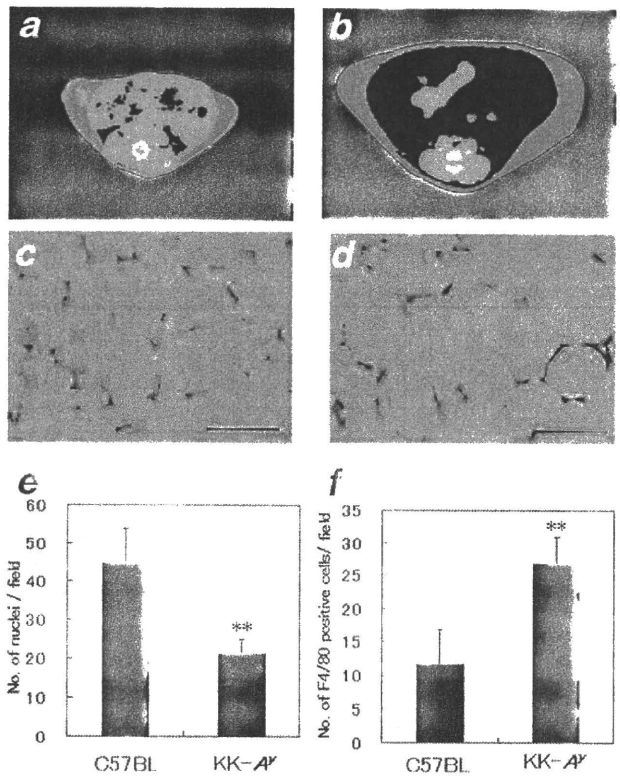

Figure 1. Obese features observed in KK-A^y mice at 13 weeks. Abdominal fat scanned by micro-CT was reconstructed to axial images (yellow represents subcutaneous fat and red represents visceral fat) for C57BL/6J (*a*) and KK-A^y mice (*b*). Histopathological sections of visceral fat in C57BL/6J (*c*) and KK-A^y mice (*d*) are also shown. Numbers of nuclei of fat cells (*e*) and F4/80 positive cells (*f*) were counted per microscopical field in visceral fat tissue as mentioned in Material and Methods section. Data are means ± SE. Bar represent 200 μm. $^{**}p < 0.01$ *vs.* C57BL/6J mice.

Increased colorectal carcinogenesis in KK-A^y mice

All KK-A^y mice and C57BL/6J mice developed ACF in the colon and rectum at 13 weeks with AOM treatment (Table 2). In spite of the treatment of both mice with AOM at the same dosage (200 μg/mouse [≈10 mg/kg], once weekly for 3 weeks), induction of colorectal ACF was much greater in KK-A^y mice compared to C57BL/6J mice. The number of total ACF in KK-A^y mice was 69.6 ± 12.9/mouse, which was almost 8 times higher than that in C57BL/6J mice. Significant numbers of colorectal ACF were observed in all portions of the colorectum in KK-A^y mice, but they were most abundant in the distal portion. The size of aberrant crypts did not differ between C57BL/6J and KK-A^y mice. Saline-treated KK-A^y and C57BL/6J mice did not develop colorectal ACF.

All of the KK-A^y mice developed colorectal tumors by AOM administration at great numbers compared with C57BL/6J mice (Table 3). Most colorectal tumors were distributed in the middle-distal portion. The color of colorectal tumors observed in KK-A^y mice was quite different from that observed in C57BL/6J mice, and the color of colorectal tumors in KK-A^y mice was intense red (Fig. 3*a*). Histopathological examination revealed AOM-induced colorectal tumors to be adenomas or adenocarcinomas. Table 3 summarizes

Table 1. Serum adipocytokine levels in KK-A^y and C57BL/6J mice treated with AOM

	13 week-old		19 week-old	
Adipocytokines	KK-A^y	C57BL	KK-A^y	C57BL
IL-6 (pg/mL)	40.4 ± 21.5**	15.9 ± 2.5	86.0 ± 57.9**	24.0 ± 6.6
Leptin (ng/mL)	34.5 ± 15.2**	1.5 ± 0.6	40.1 ± 13.4**	3.0 ± 2.9
Pai-1 (ng/mL)	3.8 ± 1.2*	2.3 ± 1.1	5.6 ± 1.8	4.1 ± 0.9
Resistin (ng/mL)	3.6 ± 0.3**	2.5 ± 0.2	4.3 ± 1.3	3.1 ± 1.0
TNF-α (pg/mL)	14.7 ± 0.7	13.4 ± 0.3	16.6 ± 2.1	16.4 ± 3.6

Data are mean ± SD. Significantly different from the C57BL/6J mice at $^{*}p < 0.05$, $^{**}p < 0.01$, respectively.

data on incidence and multiplicity. The incidence of adenoma was 84% and of adenocarcinoma was 88% in KK-A^y mice, and these values were significantly higher than those of C57BL/6J mice (8% and 4%, respectively). The number of adenoma and adenocarcinoma were 3.20 ± 3.18 and 4.60 ± 4.60 in KK-A^y mice, respectively, and were significantly higher than those of C57BL/6J mice. All adenocarcinomas in both KK-A^y mice and C57BL/6J mice were characterized by tubular structures lined by tall columnar epithelium with scant cytoplasm and enlarged euchromatic nuclei. Particularly in KK-A^y mice, remarkable tumor angiogenesis, hemorrhage and vasodilation were characteristically observed near the surfaces of adenocarcinoma (Fig. 3*b*). Moreover, invasive growth reaching into muscular layer of mucosa was found in 4 out of 22 KK-A^y mice (Fig. 3*c*). Meanwhile, such lesions were not observed in C57BL/6J mice. Metastatic lesions in the liver and other tissues were not observed in KK-A^y mice with colon adenocarcinoma. Saline-treated KK-A^y and C57BL/6J mice did not develop colorectal tumors.

To clarify the factors which have an effect on high susceptibility of KK-A^y mice to AOM-induced colorectal ACF/tumor development, length of crypt and cells/crypt in the colon were analyzed. The length of colon crypt was longer and the number of cells/crypt was higher in KK-A^y mice with AOM treatment compared with C57BL/6J mice with AOM treatment at 19 weeks (Supporting Information Table S3). Other factors such as difference of AOM metabolism were also evaluated between KK-A^y and C57BL/6J mice. To this end, activities of CYP2E1,[24] the main enzyme that metabolizes AOM, were calculated and similar CYP2E1 activities were observed between KK-A^y and C57BL/6J mice (Supporting Information Table S4).

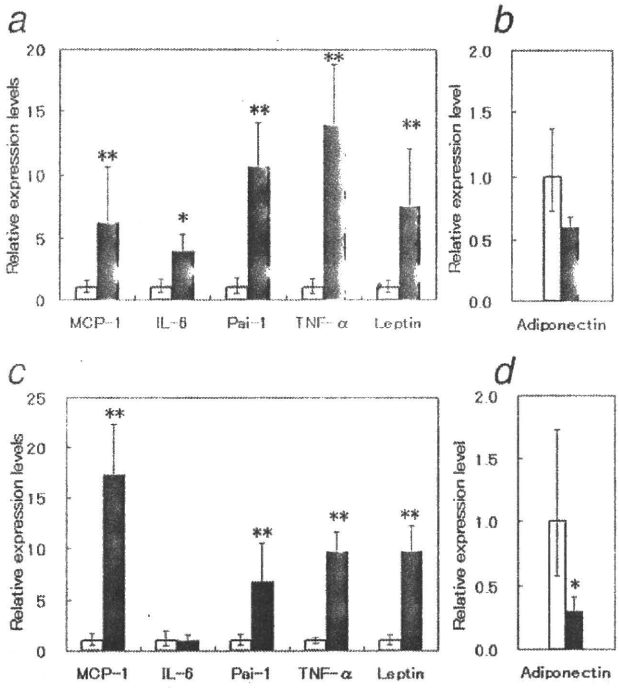

Figure 2. Relative expression levels of adipocytokine mRNA in visceral fat tissue of KK-A^y and C57BL/6J mice treated with AOM. RT-PCR analysis was performed to obtain MCP-1, IL-6, Pai-1, TNF-α, leptin and adiponectin mRNA expression levels at 13 weeks (*a* and *b*) and 19 weeks (*c* and *d*). GAPDH mRNA was used to normalize the data. KK-A^y mice (■); C57BL/6J mice (□). Data are means ± SE. $*p < 0.05$, $**p < 0.01$ *vs.* C57BL/6J mice.

Discussion

In this study, obese diabetic KK-A^y mice were found to be highly susceptible to induction of ACF, and developed colorectal carcinoma within a very short period after AOM injection. Furthermore, some of the tumors exhibited cancer cell invasion under the muscular layer of mucosa and remarkable tumor angiogenesis. The KK-A^y mouse exhibited abdominal obesity, hypertriglyceridemia and hyperinsulinemia at the time-points of colorectal ACF (13 weeks) and cancer (19 weeks) examinations, and serum pro-inflammatory adipocytokines such as IL-6, leptin and Pai-1 were also elevated compared with those in lean C57BL/6J mice. Moreover, expression of pro-inflammatory adipocytokine mRNA such as IL-6, leptin, MCP-1, Pai-1 and TNF-α was significantly increased in the visceral fat tissue; in contrast, adiponectin was decreased as reported previously.[21,25,26]

The number of ACF/mouse developed in KK-A^y mice (≈70/mouse) by AOM (200 μg/mouse [≈10 mg/kg], once weekly for 3 weeks) seems to be higher than the number of ACF/mouse developed in other obese mice, *ob/ob* mice or *db/db* mice treated with AOM. It has been reported that injection of AOM (5 mg/kg, once weekly for 4 weeks) to *ob/ob* and *db/db* mice resulted in ≈15 colorectal ACF/mouse, and to lean littermates, C57BL, resulted in ≈6 ACF /mouse.[6] High dose of AOM (15 mg/kg, once weekly for 5 weeks) to *db/db* mice were reported to be ≈30 ACF /mouse, and ≈16 ACF /mouse in their lean litter mates.[27] Up to now, studies covering colorectal cancer development in *ob/ob* or *db/db* mice

Table 2. Development of colorectal ACF in KK-A^y and C57BL/6J mice treated with AOM

		No. of ACF/colorectum					
Mice	No. of mice with ACF	Proximal	Middle	Distal	Rectum	Total	Mean no. of ACs/focus
C57BL	10/10	0.2 ± 0.4	1.6 ± 1.5	4.2 ± 1.0	3.2 ± 0.9	9.2 ± 1.3	1.8 ± 0.3
KK-A^y	10/10	12.3 ± 11.4**	20.3 ± 9.0**	30.3 ± 2.3**	6.7 ± 1.0*	69.6 ± 12.9**	1.6 ± 0.2

Data are mean ± SD. Significantly different from the C57BL/6J mice at $*p < 0.05$, $**p < 0.01$, respectively.

Table 3. Incidence and multiplicity of colorectal tumors in KK-A^y and C57BL/6J mice treated with AOM

Mice	No. of mice	No. of mice with tumors (%)			No. of tumors/mouse		
		Adenoma	Adenocarcinoma	Total	Adenoma	Adenocarcinoma	Total
C57BL	25	2 (8)	1 (4)	3 (12)	0.04 ± 0.20	0.08 ± 0.28	0.12 ± 0.33
KK-A^y	25	21 (84)**	22 (88)**	25 (100)**	3.20 ± 3.18**	4.60 ± 4.60**	7.80 ± 7.20**

Data are mean ± SD. Significantly different from the C57BL/6J mice at $^{**}p < 0.01$.

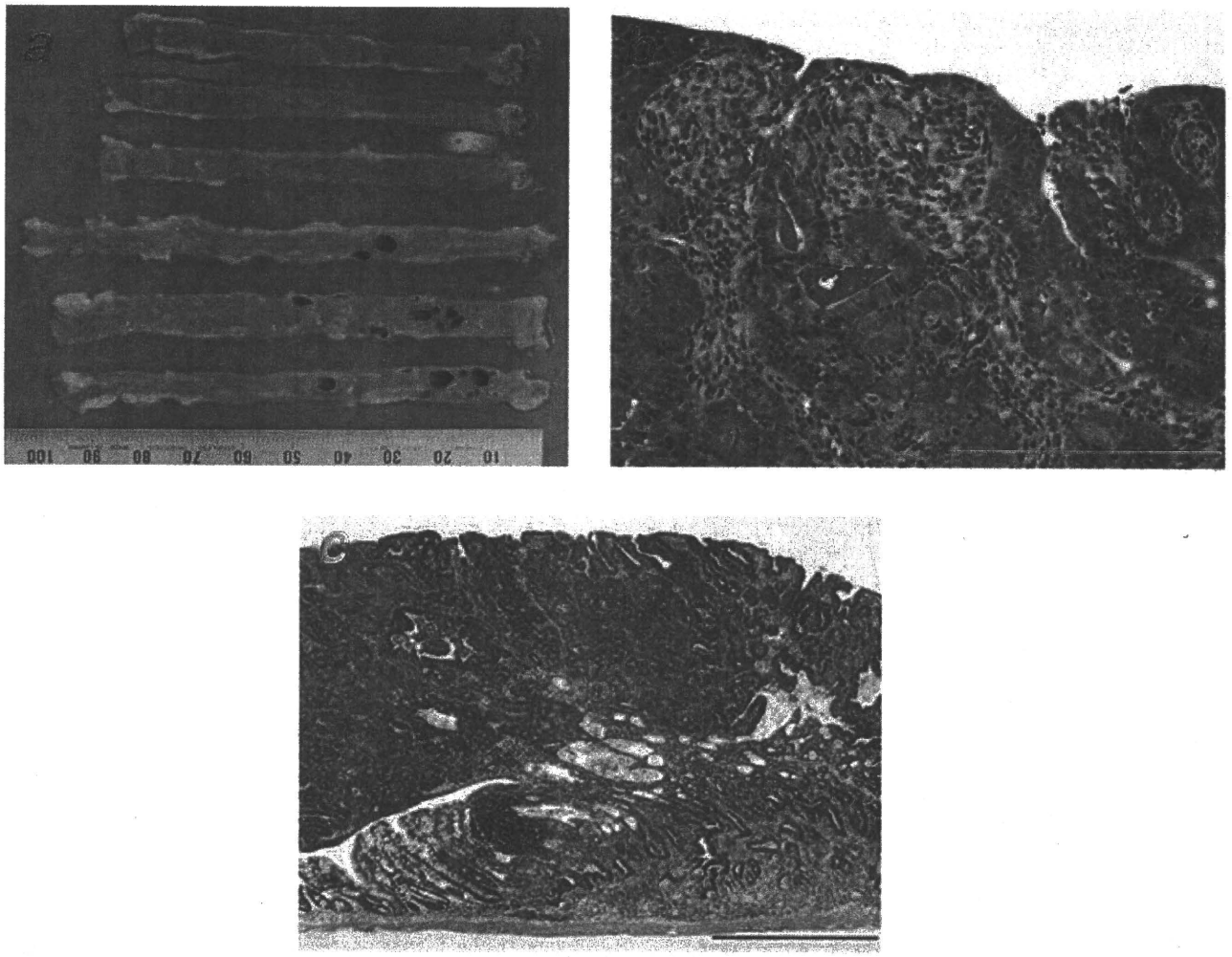

Figure 3. Macroscopic and histopathological analysis of colorectal tumors. (*a*) Representative macroscopic features of colorectal tumors developing in KK-A^y (lower three colorectal segments) and C57BL/6J mice (upper three colorectal segments) with a ruler. (*b*) Representative adenocarcinoma in KK-A^y mouse. Bar represent 200 μm. (*c*) Representative histopathologic section of adenocarcinoma showing a neck and body in KK-A^y mouse. Bar represent 500 μm.

have not been reported. In our study, we found that colorectal cancer developed in KK-A^y mice within a short period.

In well-established AOM-induced colorectal cancer study, generally it will take almost one year after 6 weekly AOM injection to develop 50–60% of colorectal cancer incidence in C57BL/6J mice.[28] Our models developed cancer within 20 weeks after AOM injection. In addition, it is worthwhile to mention that some tumors developing in KK-A^y mice showed cancer cell invasion under the muscular layer of mucosa, which are rarely observed in AOM-induced colorectal cancer in other mice strain.[29] Other characteristic features of developed colorectal cancer were its redness. Microscopic examination revealed much vessel formation and vasolidation, account for the redness of the lesions. One mechanism for enhanced tumor angiogenesis could be explained by the presence of elevated leptin and Pai-1 (Fig. 2), which promote

angiogenic signaling.[8,30] Leptin binding to Ob-Rbl induces STAT3 binding and resulted in induction of angiogenic factors, such as vascular endothelial growth factor (VEGF).[8] PAI-1 maintains extracellular matrix integrity required for endothelial cell differentiation.[31] Moreover, the expression and secretion of VEGF is insulin-dependent, and the circulating VEGF levels are increased in hyperinsulinemic state.[32]

Increased serum levels of pro-inflammatory cytokines such as Pai-1 and IL-6 or decreased adiponectin level could be derived from hypertrophic adipose tissue with invading pro-inflammatory monocyte such as activated macrophages.[33] In human beings, such a disruption of adipocytokine production is also observed in metabolic syndrome patients,[34,35] and changes of adipocytokine balance could be a clue to clarify the relationship between obesity and colorectal cancer. For instance, it has been demonstrated that TNF-α signaling blockade suppresses colorectal carcinogenesis in AOM-DSS treated mice, wherein high TNF-α expressions were observed.[34] Treatment of *Apc*-deficient mice with Pai-1 inhibitor suppressed intestinal polyp formation in which high Pai-1 expressions were observed.[22] In contrast, adiponectin knockout mice fed a high-fat diet increased the number of AOM-induced colon ACF and adenocarcimnoma.[35] These papers support the idea that high-expression levels of adipocytokines, except for adiponectin, affect the formation of colon ACF and adenocarcinoma as observed in this study. Further investigation using TNF-α blocker, Pai-1 inhibitor and adiponectin stimulator in this novel mouse model could clarify the relationship between obesity and colorectal cancer.

In conclusion, this studies indicated that KK-A^y mice exhibiting a metabolic syndrome profile are highly susceptible to AOM induced colorectal ACF/tumor development, with occurrence of tumors within a short period. Thus, the KK-A^y mouse could be a useful animal model for human obesity-associated cancer, to clarify important links between factors for the metabolic syndrome and colorectal cancer development.

We thank Ms. Misako Iio (University of Shizuoka) for technical supports. S.T. is presently the recipient of a Research Resident Fellowship from the Foundation for Promotion of Cancer Research.

Meyerhardt JA, Woodward M, Hawley R. Obesity and risk of colorectal cancer: a meta-analysis of 31 studies with 70,000 events. *Cancer Epidemiol Biomarkers Prev* 2007;16:2533–47.

Larsson SC, Wolk A. Obesity and colon and rectal cancer risk: a meta-analysis of prospective studies. *Am J Clin Nutr* 2007; 86:556–65.

Zhang Y, Proenca R, Maffei M, Barone M, Leopold L, Friedman JM. Positional cloning of the mouse obese gene and its human homologue. *Nature* 1994;372: 425–32.

Tartaglia LA, Dembski M, Weng X, Deng N, Culpepper J, Devos R, Richards GJ, Campfield LA, Clark FT, Deeds J, Muir C, Sanker S, et al. Identification and expression cloning of a leptin receptor, OB-R. *Cell* 1995;83:1263–71.

Takaya K, Ogawa Y, Isse N, Okazaki T, Satoh N, Masuzaki H, Mori K, Tamura N, Hosoda K, Nakao K. Molecular cloning of rat leptin receptor isoform complementary DNAs—identification of a missense mutation in Zucker fatty (*fa/fa*) rats. *Biochem Biophys Res Commun* 1996;255: 75–83.

Ealey KN, Lu S, Archer MC. Development of aberrant crypt foci in the colons of *ob/ob* and *db/db* mice: evidence that leptin is not a promoter. *Mol Carcinog* 2008;47: 667–77.

Lee WM, Lu S, Medline A, Archer MC. Susceptibility of lean and obese Zucker rats to tumorigenesis induced by *N*-methyl-*N*-nitrosourea. *Cancer Lett* 2001;162:155–60.

Garofalo C, Surmacz E. Leptin and cancer. *J Cell Physiol* 2006;207:12–22.

Kondo K, Nozawa K, Romida T, Ezaki K. Inbred strains resulting from Japanese mice. *Bull Exp Anim* 1957;6:107–12.

Nakamura M, Yamada K. Studies on diabetic KK strain of the mouse. *Diabetologia* 1967;3:212–21.

Suto J, Matsuura S, Imamura K, Yamanaka H, Sekikawa K. Genetic analysis of non-insulin dependent diabetes mellitus in KK and KK-A^y mice. *Eur J Endocrinol* 1998;139:654–61.

Kato H, Ohue M, Kato K, Nomura A, Toyosawa K, Furutani Y, Kimura S, Kadowaki T. Mechanism of amelioration of insulin resistance by beta3-adrenoceptor agonist AJ 9677 in the KK-A^y/Ta diabetic obese mouse model. *Diabetes* 2001;50: 113–22.

Shiuchi T, Iwai M, Li HS, Wu L, Min LJ, Li JM, Okumura M, Cui TX, Horiuchi M. Angiotensin II type-1 receptor blocker valsartan enhances insulin sensitivity in skeletal muscles of diabetic mice. *Hypertension* 2004;43:1003–10.

Gohda T, Tanimoto M, Kaneko S, Shibata T, Funabiki K, Horikoshi S, Tomino Y. Minor gene effect of leptin receptor variant on the body weight in KK/Ta mice. *Diabetes Obes Metab* 2006; 8:581–4.

Mutoh M, Watanabe K, Kitamura T, Shoji T, Takahashi M, Kawamori T, Tani K, Kobayashi M, Maruyama T, Kobayashi K, Ohuchida S, Sugimoto Y, et al. Involvement of prostaglandin E receptor subtype EP$_4$ in colon carcinogenesis. *Cancer Res* 2002;62:28–32.

Pozharisski KM. Tumours of the intestines. In: Turusov VS, ed. Pathology of tumours in laboratory animals. IARC Scientific Publications no. 1. Lyon: IARC, 1973. 119–40.

Niho N, Takahashi M, Shoji Y, Takeuchi Y, Matsubara S, Sugimura T, Wakabayashi K. Dose-dependent suppression of hyperlipidemia and intestinal polyp formation in Min mice by pioglitazone, a PPARγ ligand. *Cancer Sci* 2003;94:960–4.

Fan W, Yanase T, Nomura M, Okabe T, Goto K, Sato T, Kawano H, Kato S, Nawata H. Androgen receptor null male mice develop late-onset obesity caused by decreased energy expenditure and lipolytic activity but show normal insulin sensitivity with high adiponectin secretion. *Diabetes* 2005;54:1000–8.

Inukai K, Nakashima Y, Watanabe M, Tanaka N, Sawa T, Kurihara S, Awata T, Katayama S. Regulation of adiponectin receptor gene expression in diabetic mice. *Am J Endocrinol Metab* 2005;288:E876–82.

Pan W, Hsuchou H, Tu H, Kastin AJ. Developmental changes of leptin receptors in cerebral microvessels: unexpected relation to leptin transport. *Endocrinology* 2008;149:877–85.

Abe M, Matsuda M, Kobayashi H, Miyata Y, Nakayama Y, Komuro R, Fukuhara A, Shimomura I. Effects of statins on adipose tissue inflammation: their inhibitory effect on MyD88-independent IRF3/IFN β